The Toarcian Oceanic Anoxic Event (Early Jurassic) in the Neuquén Basin, Argentina: A Reassessment of Age and Carbon Isotope Stratigraphy

Aisha H. Al-Suwaidi,[1,] Stephen P. Hesselbo,[2] Susana E. Damborenea,[3] Miguel O. Manceñido,[3] Hugh C. Jenkyns,[4] Alberto C. Riccardi,[3] Gladys N. Angelozzi,[5] and François Baudin[6]*

1. Petroleum Geoscience Department, Petroleum Institute University and Research Centre, PO Box 2533, Abu Dhabi, United Arab Emirates; 2. Camborne School of Mines, College of Engineering, Mathematics and Physical Sciences, University of Exeter, Penryn Campus, Penryn, Cornwall TR10 9FE, United Kingdom; 3. División Paleozoología Invertebrados, Facultad de Ciencias Naturales y Museo, Universidad Nacional de La Plata, Argentina, Paseo del Bosque S/N, 1900 La Plata, Argentina; and Consejo Nacional de Investigaciones Científicas y Técnicas; 4. Department of Earth Sciences, University of Oxford, South Parks Road, Oxford OX1 3AN, United Kingdom; 5. Laboratorio de Bioestratigrafía, Área de Geociencias, YPF Tecnología, Baradero S/N, 1925 Ensenada, Argentina; 6. Université Pierre et Marie Curie (UPMC–Université de Paris 06), Institut des Sciences de la Terre de Paris (ISTeP), 4 place Jussieu, Paris, France

ABSTRACT

The Toarcian oceanic anoxic event (T-OAE) is recorded by the presence of globally distributed marine organic carbon–rich black shales and a negative carbon isotope shift, with $\delta^{13}C_{org}$ values as low as −33‰, interrupting an overarching positive excursion. Here we present new biostratigraphic data and high-resolution $\delta^{13}C_{org}$ data from two Southern Hemisphere localities: Arroyo Serrucho in the north and Arroyo Lapa in the south of the Neuquén Basin, Argentina. Previous studies at these localities aimed to provide an accurate numerical age for the T-OAE and characterization of its carbon isotope stratigraphy. The new carbon isotope data and ammonite biostratigraphy presented here from Arroyo Serrucho show the T-OAE to be recorded lower in the section than supposed by previous authors, thus calling into question the published age of the T-OAE in this section. A newly investigated exposure at Arroyo Lapa North shows a complex carbon isotope record with at least three high-amplitude fluctuations in the *hoelderi* zone (equivalent to the *serpentinum* zone in northwestern Europe), with $\delta^{13}C_{org}$ values of <−28‰, and two intervening positive isotope excursions, with $\delta^{13}C_{org}$ values around −24‰. At Arroyo Lapa South, the characteristic major stepped negative carbon isotope excursion is recorded, with $\delta^{13}C_{org}$ values of <−30‰ and total organic-carbon contents increasing to 11%; above this level an erosional surface of a submarine channel truncates the section. These new data are globally correlative and unambiguously illustrate the global reach of the T-OAE.

Online enhancements: supplementary data, tables, and figures.

Introduction

The changes in the carbon isotope composition of organic matter and carbonate in terrestrial and marine sediments over time indicate that the Mesozoic Era was subject to abrupt and substantial disturbances to the global carbon cycle. These carbon isotope excursions (CIEs) are associated with extreme global environmental change and commonly correspond in timing to the formation of large igneous provinces (LIPs), changes in seafloor spreading rates, possible dissociation of methane hydrate, ocean acidification, and widespread deposition of marine organic-rich black shales (e.g., Hesselbo et al. 2000;

Manuscript received February 21, 2015; accepted November 9, 2015; electronically published March 14, 2016.

* Author for correspondence; e-mail: aalsuwaidi@pi.ac.ae.

[The Journal of Geology, 2016, volume 124, p. 171–193] 0022-1376/2016/12402-0002$15.00. DOI: 10.1086/684831

Pálfy and Smith 2000; Jones and Jenkyns 2001; Jenkyns 2003, 2010; McElwain et al. 2005; Coffin et al. 2006; Wignall et al. 2006; Svensen et al. 2007; Kump et al. 2009; Percival et al. 2015). Levels of organic-carbon enrichment in particular have been linked to episodes of oxygen depletion in extensive water masses and are referred to as oceanic anoxic events, or OAEs (Schlanger and Jenkyns 1976). Three major OAEs have been identified during the Mesozoic: at the Cenomanian-Turonian boundary (~93.5 Ma), in the early Aptian (~120 Ma), and in the early Toarcian (~183 Ma), although many lesser events with more parochial sedimentary records also occurred during the Mesozoic Era (Jenkyns 2010).

Carbon isotope stratigraphy commonly shows broad positive $\delta^{13}C$ excursions over OAE intervals, interpreted as due to increased global burial rates of organic matter in the oceans. However, large negative $\delta^{13}C$ excursions punctuate both the Toarcian and Aptian events, indicating fluxes of isotopically light carbon into the ocean and atmosphere. Such carbon may be volcanically derived carbon dioxide, methane coming from dissociation of gas hydrates, thermal metamorphism of coals or black shales, or a combination thereof (e.g., Hesselbo et al. 2000; Jahren et al. 2001; Beerling et al. 2002; Jenkyns 2003, 2010; McElwain et al. 2005; Svensen et al. 2007; Méhay et al. 2009). With all OAEs there are, however, significant open questions as to how widespread was the marine anoxia/euxinia and in what basinal settings deoxygenation was favored (e.g., Pancost et al. 2004; Monteiro et al. 2012; Owens et al. 2013), hence the necessity to identify and document the expression of OAEs in globally distributed locations.

This study focuses on the Toarcian OAE (T-OAE), which is characterized by apparently coeval, globally distributed organic-rich black shale (fig. 1) deposited in oxygen-depleted marine waters (Jenkyns 1988). The T-OAE is also characterized by a large negative CIE within an overarching positive excursion. In the core of the negative excursion, values of $\delta^{13}C_{org}$ as low as −28.5‰ to −33‰ are recorded in both fossil wood and marine organic matter from Europe, North America, Siberia, and Japan (e.g., Küspert 1982; Jenkyns and Clayton 1986, 1997; Hesselbo et al. 2000, 2007; Schouten et al. 2000; Röhl et al. 2001; Schmid-Röhl et al. 2002; Jenkyns 2003; Kemp et al. 2005; Hermoso et al. 2009; Sabatino et al. 2009; Bodin et al. 2010; Caruthers et al. 2011; Gröcke et al. 2011; Hesselbo and Pieńkowski 2011; Kafousia et al. 2011; Suan et al. 2011; Kemp and Izumi 2014).

Two studies regarding the expression of the T-OAE in the Neuquén Basin, Argentina, have been published to date: one focused on carbon isotope stratigraphy and biostratigraphy at Arroyo Lapa, Neuquén Province (Al-Suwaidi et al. 2010), and the other on carbon isotope stratigraphy and radiometric ages of ash beds from Arroyo Serrucho, Mendoza Province (Mazzini et al. 2010). Mazzini et al. (2010) provided U-Pb ages of 181.42 ± 0.24 and 180.59 ± 0.43 Ma, determined by isotope-dilution TIMS on zircons from two tuff beds that they interpreted as

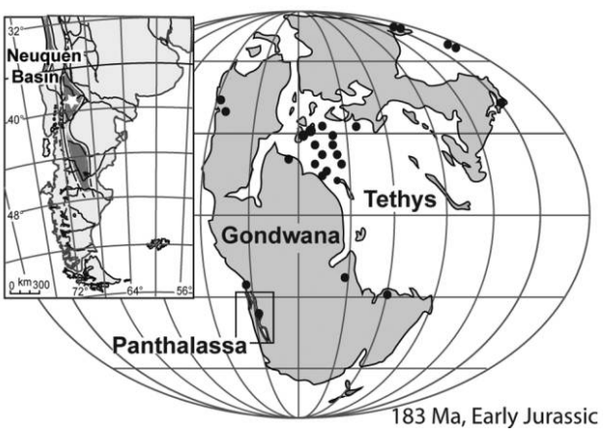

Figure 1. Global Toarcian ~183 Ma paleogeography (after Blakey 2007), showing location of organic-rich shales (black circles). Most of these localities are dated in the *tenuicostatum* and/or *falciferum* ammonite zones, corresponding to the lower Toarcian stage. Gray shading indicates continents, and white is for undifferentiated marine environments (adapted and modified after Jenkyns 1988; Jenkyns et al. 2001, 2002; Blakey 2007). *Inset*: Argentinian paleogeography (after Vicente 2005) with interior seaway; location of the Neuquén Basin is indicated by a star. Present-day latitudes and longitudes are shown on the inset map, while the paleogeographic map shows paleolatitudes.

located within the negative CIE of the T-OAE. Multiple authors have subsequently used these numerical ages to constrain the age of the timing of the T-OAE and to indicate a link between rapid emplacement of magma in Karoo and the T-OAE (e.g., Svensen et al. 2012; Leanza et al. 2013; Ikeda and Tada 2014). Here we present new data from Arroyo Lapa and Arroyo Serrucho, comprising high-resolution lithostratigraphy, biostratigraphy, organic-carbon isotopes (bulk sediment and fossil wood), total organic carbon (TOC), and hydrogen index (HI). The results give new insight into carbon isotope chemostratigraphy and biostratigraphy from the lower Toarcian in the Southern Hemisphere and, in particular, provide new stratigraphic context for the previously published radiometric ages.

Geological Setting of the Neuquén Basin

The Neuquén Basin is located in west-central Argentina, on the eastern side of the Andes, at present between 32° and 41°S latitude, with a paleolatitude during the early Jurassic of ~35°–45°S (figs. 1, 2; Franzese et al. 2003), although Iglesia Llanos et al. (2006) placed the basin at around 25°S during the Pliensbachian on the basis of paleomagnetism. This depocenter was a back-arc basin with a fill of at least 7 km of Triassic to Cenozoic deposits (Vergani et al. 1995). The basin has a multiphase tectonic history related to the breakup of Gondwana, the subduction of the proto–Pacific Plate, and the development of the Andean magmatic arc (Vergani et al. 1995). During the Early Jurassic to Early Cretaceous, regional back-arc extension and thermal subsidence took place, resulting in marine transgression and a general deepening. During the Jurassic, the Neuquén Basin was partially restricted on its western side by an active volcanic island arc, the Chilean Coastal Cordillera (Riccardi 1983; Digregorio et al. 1984); the arc volcanism is generally thought to have intermittently disrupted exchange of marine waters from Panthalassa, although connection continued through an opening in the northern part of the basin (Vicente 2005).

Sediment entered the Neuquén Basin from two main source areas. The Chilean Coastal Cordillera supplied immature volcaniclastic material (Caminos et al. 1982; Coira et al. 1982; Ramos et al. 1982; Eppinger and Rosenfeld 1996), whereas sediment of a more mature aspect was supplied from cratonic areas to the south and northeast, with a mixture of the two being deposited in many locations (Burgess et al. 2000; Franzese et al. 2003). Figure 2 shows the main Pliensbachian to Toarcian depositional tracts and the location within these tracts of the study sites.

Methods

At Arroyo Lapa, two adjacent sections on the northern and southern sides of the Lapa stream were examined, referred to here as Arroyo Lapa North and Arroyo Lapa South (fig. 3). In the Arroyo Lapa North section, bulk-sediment samples were collected at 10-cm intervals, wherever possible, and a total of 34 fossil wood samples were recovered from bulk-rock samples. A 50-cm-resolution record has been published for the lower part of the section at Arroyo Lapa South (Al-Suwaidi et al. 2010). In the present study, Arroyo Lapa South was sampled for bulk sediment at 10-cm intervals through the upper *tenuicostatum* and *hoelderi* ammonite zones. This new high-resolution sample set was collected from the level equivalent to 54 m in Al-Suwaidi et al. (2010), approximately 7 m below the *tenuicostatum-hoelderi* ammonite zone boundary, and continues upward for an additional ~24 m. In addition, a total of 52 wood fragments were recovered from bulk-rock samples.

In the Arroyo Serrucho section (fig. 4), samples come from three subsections: A–A′ (~49 m), B–B′ (~14 m), and C–C′ (~28 m). Samples from A–A′ and B–B′ were collected at 50-cm intervals, wherever possible, and include a total of 6 fossil wood fragments. Bulk-sediment samples from section A–A′ were collected up to 32.5 m because of limited outcrop exposure above this level, although ammonites were sampled to ~49 m. Section C–C′ was examined in 2008, when bulk sediment and fossil wood samples were collected for organic-carbon isotopes up to 8.7 m; an additional 20 m was logged and sampled for biostratigraphy in 2014.

In all sections, ammonites and other fossils (e.g., bivalves and brachiopods) were sampled wherever found, and bulk-rock samples were collected at 1-m intervals for nannofossils. Detailed sample locations and biostratigraphic determinations of fossils are given in the supplementary files available online. Ammonites have been referred to a biostratigraphic zonation valid for the whole Andean region of Argentina and Chile (fig. 5; von Hillebrandt et al. 1992; Riccardi 2008*a*, 2008*b*). A multiple-zone scheme based on ammonites, bivalves, brachiopods, and calcareous microfossils has also been established for the Neuquén Basin (Riccardi et al. 2000, 2011).

Collected samples were processed for TOC, HI, and carbon isotope ratios ($\delta^{13}C_{org}$). The TOC was measured by total carbon combustion with a Strohlein

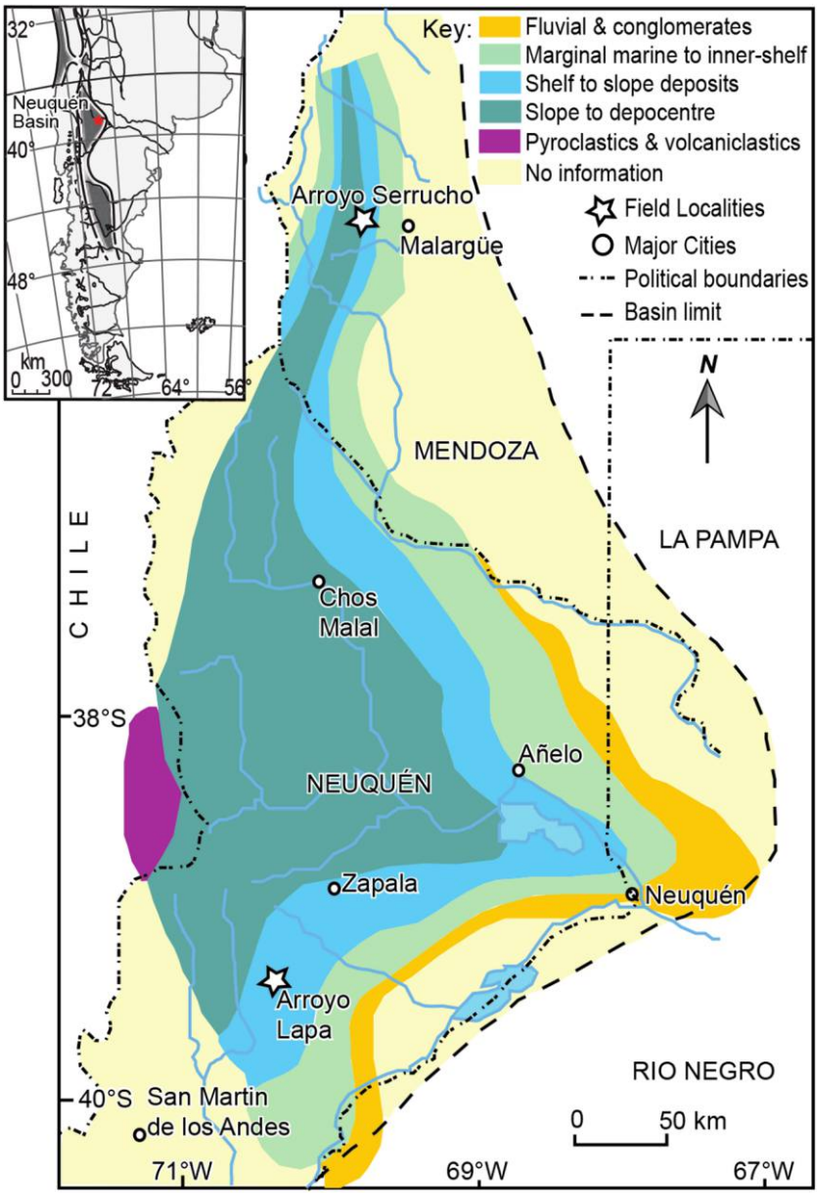

Figure 2. Map of the Neuquén Basin (red star in inset), showing Pliensbachian to Toarcian depositional tracts within the basin. Stars indicate field localities examined in this study. Map adapted from Riccardi et al. (2011), modified from Legarreta and Uliana (1996).

Coulomat 702 SO/CS at the University of Oxford (details in Jenkyns 1988). Stable carbon isotopes were measured in both decarbonated bulk sediment and fossil wood. Samples were treated with 3M HCl for 24 h to remove calcium carbonate and sulfur compounds; the samples were shaken every few hours to increase the reaction surface area and prevent sediment settling. After 24 h, the samples were centrifuged and the HCl decanted. A second addition of HCl was made, and the sample was shaken. If any resulting effervescence was observed (suggesting the presence of surviving calcium carbonate), the sample was treated with HCl again until no more effervescence was observed. Clear, carbonate-free samples were rinsed with deionized water until clear and neutral and dried in an oven overnight at 60°C. Samples were analyzed in the Research Laboratory for Archaeology and Art History at the University of Oxford with a Carlo Erba Elemental Analyser coupled to a Europa Scientific CN biological sample

Figure 3. *A*, Satellite image (courtesy of Google Earth Pro, ver. 7.1.1.1888; Sept. 1, 2013) of the Arroyo Lapa field locality in the Sierra de Chacaico area, Neuquén Province, Argentina: lat 39°24′04.87″S, long 70°25′43.21″W, elevation 1311 m. Image indicates the locations of Arroyo Lapa North and South sections measured and sampled in 2010, which are indicated by solid black lines. The dashed black line indicates the 2008 section published in Al-Suwaidi et al. (2010). *B*, Photograph showing the main trenched section at Arroyo Lapa South. *C*, Photograph of the upper part of Arroyo Lapa North. A color version of this figure is available online.

converter connected to a Geo 20-20 stable-isotope gas-ratio mass spectrometer, and at the University of Kansas Keck laboratory with a high-temperature conversion elemental analyzer coupled to a Thermofinnigan MAT 253. Samples from Arroyo Lapa North and South were also analyzed via ROCK EVAL III oil show analyzer pyrolysis at the Institut des Sciences de la Terre de Paris, Université Pierre et Marie Curie, to determine the source and degree of thermal maturation of the organic matter in bulk-sediment samples. All chemostratigraphic data are available in a supplementary file, available online.

Lithologic and Biostratigraphic Framework

The Arroyo Lapa locality lies on the eastern slope of Sierra de Chacaico anticline, about 50 km southwest of the town of Zapala in Neuquén Province. The overall succession comprises about 900 m of upper Triassic–lower Jurassic strata, made up of up-

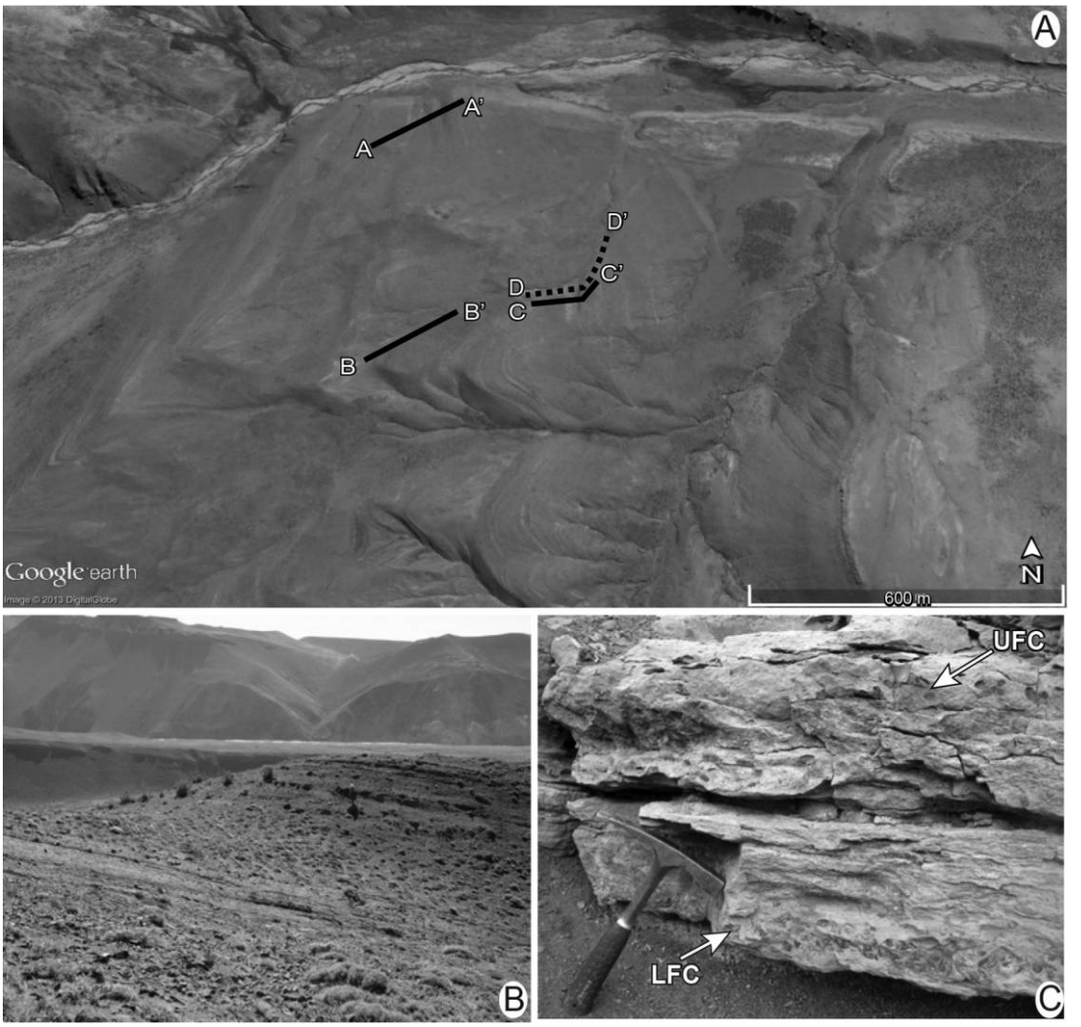

Figure 4. *A*, Satellite image (courtesy of Google Earth Pro, ver. 7.1.1.1888; Sept. 1, 2013) of the Arroyo Serrucho field locality in Mendoza Province, Argentina: lat 35°26′24″S, long 69°53′59″W, elevation 2299 m. Image indicates the location of sections A–A′, B–B′, C–C′, which are denoted by solid black lines. The Mazzini et al. (2010) section, D–D′, is indicated with a dashed black line. *B*, Photograph showing overview of section B–B′. *C*, Photograph showing the location of a surface with attributes of extreme condensation or hiatus at Arroyo Serrucho (equivalent to the layer at ~6 m of section C–C′). White arrows indicate the location of the lower fossil conglomerate (LFC) and the upper fossil conglomerate (UFC), wood, steinkern, and phosphate nodule levels. A color version of this figure is available online.

permost Triassic–Hettangian pyroclastic deposits of the Lapa Formation and Pliensbachian-Aalenian outer-shelf to basinal shale and sandstone of the Los Molles Formation (Gulisano and Gutiérrez Pleimling 1995*a*). The succession reported in detail here lies within the Los Molles Formation (fig. 5). Previous stratigraphic studies at Arroyo Lapa have documented nannofossils and ammonites (von Hillebrandt 1973, 1987, 2006; von Hillebrandt and Schmidt-Effing 1981; Al-Suwaidi et al. 2010), teuthids (Riccardi 2005), palynomorphs (Volkheimer 1973), bivalves (Damborenea 1987*a*, 1987*b*, 1989, 2002), and paleomagnetic data (Iglesia Llanos and Riccardi 2000).

The two sections at Arroyo Lapa are on the north and south sides of the Lapa stream, ~400 m apart (fig. 3). Initial lithostratigraphic, sedimentologic, biostratigraphic, and chemostratigraphic results from Arroyo Lapa South have been reported in Al-Suwaidi et al. (2010). Here we present an extended and more detailed analysis of the upper part of the same section, together with new data from Arroyo Lapa North.

Arroyo Lapa North

Arroyo Lapa North is located on the northern side of Lapa stream (fig. 3). This section is ~30 m thick and

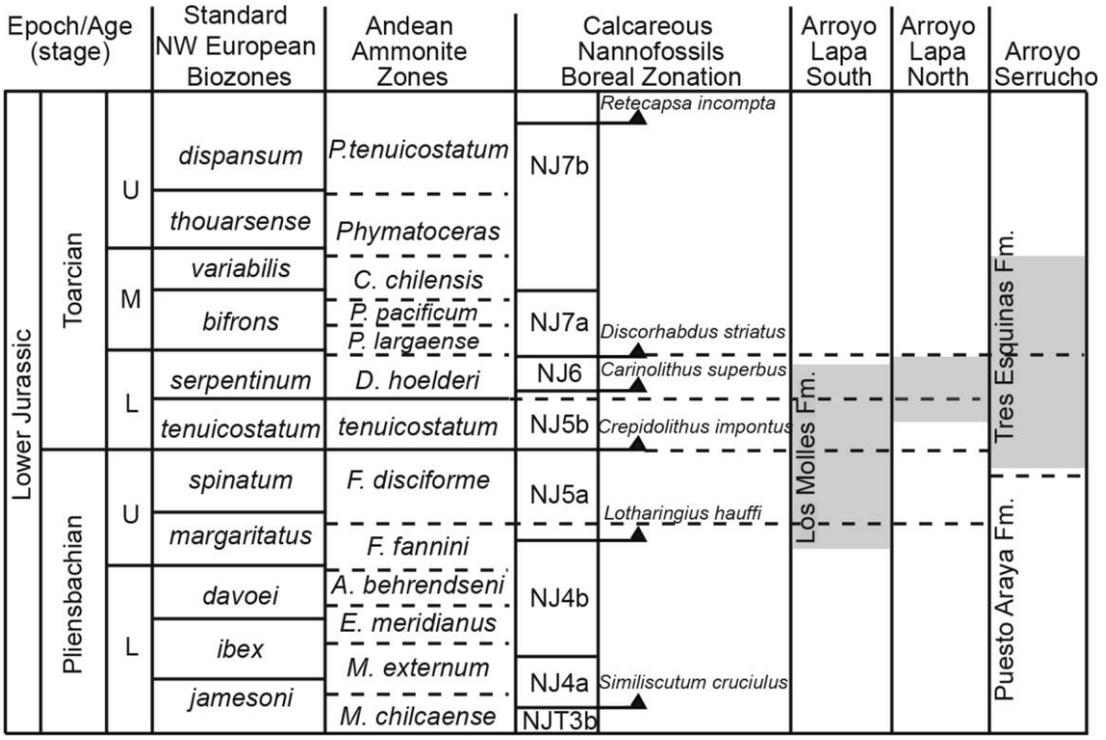

Figure 5. Table showing the epoch/age, standard northwestern (NW) European biozones (Page 2004), biostratigraphy (ammonites and nannofossils), and an overview of the three field localities examined in this study, indicating stratigraphic and biostratigraphic intervals present within the studied sections (shaded areas). Ammonite biostratigraphy is adapted from Riccardi (2008*a*, 2008*b*), and nannofossils, chronozones, and epoch/age are adapted from Gradstein et al. (2012). U = upper; M = middle; L = lower. *P. tenuicostatum* = ?*Phlyseogrammoceras tenuicostatum*; *C. chilensis* = *Collina chilensis*; *P. pacificum* = *Peronoceras pacificum*; *P. largaense* = *Peronoceras largaense*; *D. hoelderi* = *Dactylioceras hoelderi*; *F. disciforme* = *Fanninoceras disciforme*; *F. fannini* = *Fanninoceras fannini*; *A. behrendseni* = *Austromorphites behrendseni*; *E. meridianus* = *Eomaltheus meridianus*; *M. externum* = *Meridiceras externum*; *M. chilcaense* = *Miltoceras chilcaense*. Fm. = Formation.

is separated by an exposure gap of 3.8 m into lower (~4.3 m) and upper (~22 m) parts. The base of the section in figure 6 comprises ferruginous cemented sandstone and is overlain by siltstone and mudstone interbedded with very fine-grained sandstone. The upper part of the section similarly comprises siltstone and mudstone interbedded with fine- to very fine-grained sandstone. Ammonites, bivalves, and fossil wood are common throughout. The sand content increases significantly upward in the section, culminating in cross-laminated fine-grained sandstone, with abundant wood fragments, which forms a prominent topographic ridge.

The biostratigraphic determinations confirm an early Toarcian age. The base of the section is in a zone of uncertainty (<14.50 m) and includes lowest occurrences (LwOs) of ammonites and nannofossils indicative of the early Toarcian *tenuicostatum* to *hoelderi* ammonite zones. Nannofossils such as *Biscutum finchii* (Crux) (LwO 10.80 m) and the highest occurrence of *Lotharingius hauffi* Grün and Zwili (14.50 m) are characteristic of the latest Pliensbachian and earliest Toarcian in Europe (Mattioli and Erba 1999; Fraguas and Young 2011), while ammonites such as ?*Hildaites* sp. (LwO 9.50 m; cf. Howarth 1992) are characteristic of the early Toarcian. The Andean *hoelderi* zone is approximately equivalent to the *serpentinum* (=*falciferum*) ammonite zone of northwestern Europe (von Hillebrandt and Schmidt-Effing 1981; Page 2004; Riccardi 2008*a*, 2008*b*). Ammonites from the Andean *hoelderi* zone occur from 14.50 m upward, as indicated by the LwO of *Hildaites* cf. *murleyi* (Moxon) (cf. von Hillebrandt 1987; Howarth 1992, p. 168; Riccardi et al. 2011), as well as the occurrence of the nannofossil *Orthogonoides hamiltoniae* (Wiegand) (LwO 14.90 m) and *Calyculus* sp. (LwO 24.30 m).

Arroyo Lapa South

The Arroyo Lapa South section in this study overlaps the upper 17 m of the section published in

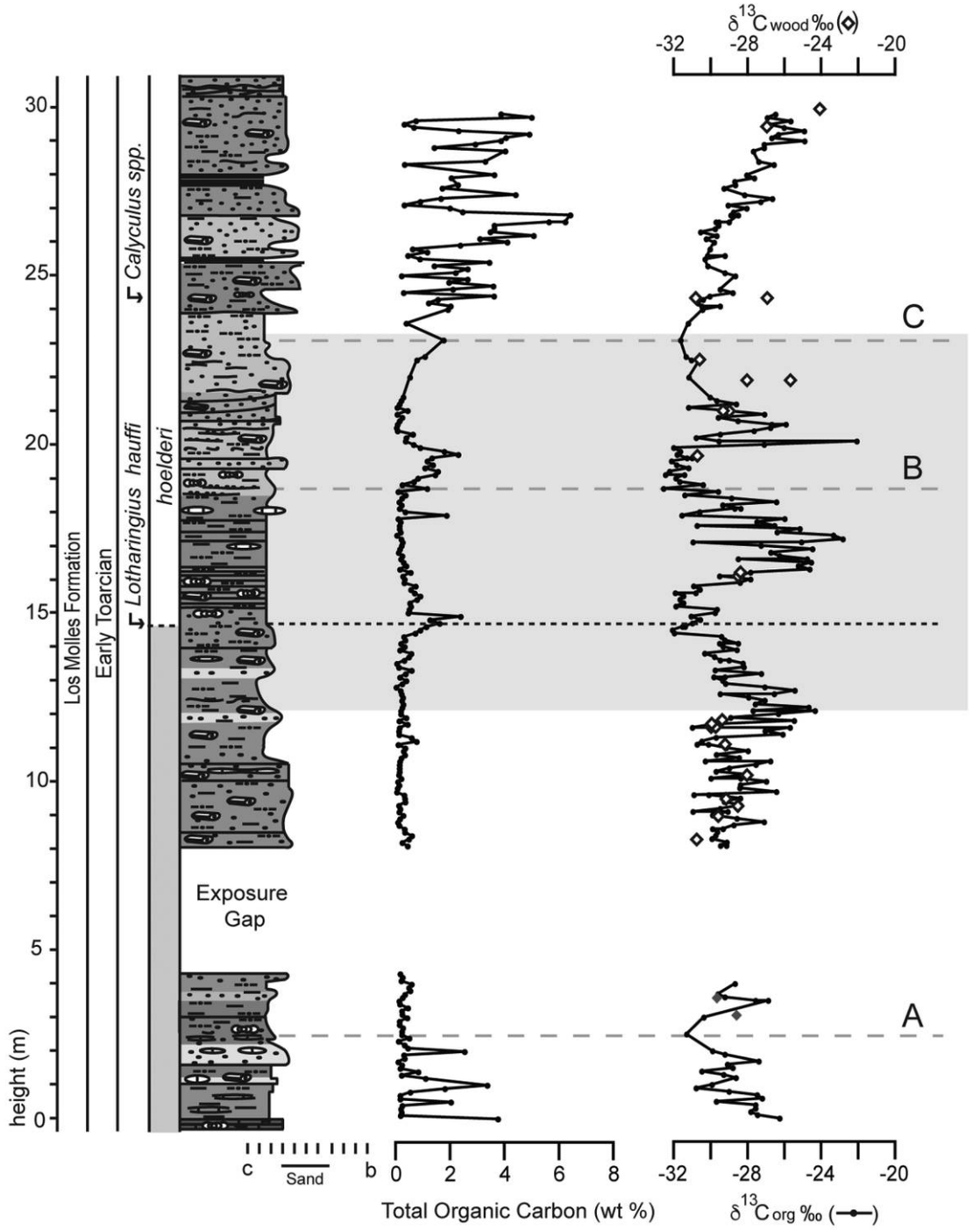

Figure 6. Section at Arroyo Lapa North, showing $\delta^{13}C_{org}$ from bulk sediment and wood (diamonds) and total organic carbon profile. The short-dashed line indicates the lowest occurrence of ammonites in the *hoelderi* Andean ammonite zone. The shaded box indicates the Toarcian oceanic anoxic event and associated carbon isotope excursion. Note the negative 6‰–7‰ excursion in the $\delta^{13}C_{org}$ from bulk sediment leading to the top of the *tenuicostatum* zone, followed by a short-lived positive excursion of 6‰ at ~16 m. There is a return to more isotopically light values as well as a second negative excursion of 6‰ in the *hoelderi* zone (level B), followed by a positive recovery at the top of the section (level C). Gray long-dashed lines labeled A–C are referred to in the text. The column on the left-hand side of the figure indicates lithostratigraphy, stage, lowest nannofossil occurrence, Andean ammonite zone, and the simplified graphical log for Arroyo Lapa North. Detailed key of lithologies and other key elements are as given in figure 8.

Al-Suwaidi et al. (2010) and extends upward an additional 7 m. The position of the *tenuicostatum-hoelderi* ammonite zone boundary has also been refined.

The base of the section in figure 7 comprises laminated fine- to very fine-grained sand, with poorly sorted, abundant wood fragments. Above this unit, the section comprises laminated black shale and siltstone interbedded with very fine-grained and tuffaceous sandstone. Ammonites, bivalves, and fossil wood are common throughout the section. A clast-supported oligomictic conglomerate with a muddy matrix occurs at ~15 m, equivalent to the level at 70 m in Al-Suwaidi et al. (2010). Pebbles, cobbles, and boulders composed of a large variety of igneous and sedimentary rock types are mixed with corals, ammonites, and fossil wood fragments. Some boulders are encrusted with bivalves.

The LwO of confidently identified *Dactylioceras* (?*Eodactylites*) sp. is at 0.6 m (equivalent to 54.5 m in Al-Suwaidi et al. 2010), suggesting that the Pliensbachian-Toarcian boundary may be located at (or slightly below) this level. The only other ammonite indicative of the *tenuicostatum* ammonite zone occurring at a stratigraphically lower position is ?*Dactylioceras* sp., which occurs ~10 m below the base of the section, equivalent to 46.05 m in Al-Suwaidi et al. (2010).

The *tenuicostatum-hoelderi* ammonite zonal boundary is now placed between ~6.5 and 7.2 m, as marked by the LwO of *Harpoceras* cf. *serpentinum* (Schlotheim), at 6.9 m. Other identified ammonites through the Arroyo Lapa South section that are indicative of the *hoelderi* ammonite zone include *Dactylioceras* (*Orthodactylites*) cf. *hoelderi* (von Hillebrandt and Schmidt-Effing 1981; LwO 7.8 m) and *Hildaites* cf. *murleyi* (Moxon) (cf. von Hillebrandt 1987; Howarth 1992, p. 168; Riccardi et al. 2011; LwO 9.70 m). There are three bivalve species in the Arroyo Lapa South section that have a range limited to the latest Pliensbachian to earliest Toarcian, including *Entolium mapuche* Damborenea (LwO 13.1 m) and *Weyla alata angustecostata* (Philippi; LwO 13.6 m); the bivalve *Posidonotis cancellata* (Leanza) is present throughout most of the section and has a range limited to the latest Pliensbachian to earliest Toarcian (Damborenea 2002).

The deposits at Arroyo Lapa North and South are assumed to be a part of the same depositional system, given the close proximity of these two sections. Turbidite deposits, with coarse-grained sandstone bases, grading to fine mudstone units, dominate both sections. The presence of thin, relatively unreworked tuffaceous material throughout the sections suggests close proximity to a volcanic source area. Burgess et al. (2000) examined the sandstone petrographically and confirmed the presence of rather immature volcaniclastics, suggesting close proximity to an adjacent volcanic system. Deposits of beds rich in charcoalified wood indicate that the sections at Arroyo Lapa were also relatively close to a continental source of sediment.

Gulisano and Gutiérrez Pleimling (1995*a*) interpreted the turbiditic part of the section at Arroyo Lapa South as representing deposits from channel-levee submarine-fan complexes, including finer-grained overbank deposits. This channel-levee complex may account for the difference in sediment type between Arroyo Lapa South and Arroyo Lapa North. Arroyo Lapa North has significantly more coarse-grained sandy material and woody debris, suggesting dominance of levee deposits. In Arroyo Lapa South, the sediments are typically fine-grained sands and shales and may represent dominance of overbank deposits. However, the fossil-rich conglomerate bed at Arroyo Lapa South (15 m; fig. 7) is laterally discontinuous and probably derives from the base of a channel that migrated within the fan complex (cf. Richards et al. 1998; Bouma 2000).

Gulisano and Gutiérrez Pleimling (1995*a*) hypothesized that the deposits at Arroyo Lapa represent transgressive-regressive marine cycles, with a decrease in sandy-turbiditic units during transgression and marine highstand in the basin, although they examined an area much larger than that included in this study. The other possible reason for a decrease in sand content could be a change in the grain size of the feeder system, as suggested by Burgess et al. (2000). The variation in deposition from sandy material to fine-grained shales and back to sandier material at Arroyo Lapa North and South suggests that the basin underwent marine transgression, recording deeper marine sedimentation during relative sea level rise, in the *tenuicostatum-hoelderi* ammonite zones and more marginal marine turbiditic deposits, with increased plant material, during basin regression and the relative sea level fall later in the *hoelderi* ammonite zone.

Arroyo Serrucho

The Arroyo Serrucho section is located about 30 km west of Malargüe, Mendoza Province (figs. 2, 4; Gulisano and Gutiérrez-Pleimling 1995*b*; Nullo et al. 2005). The focus of our study is the Tres Esquinas Formation of latest Pliensbachian to Bajocian age (fig. 5), which has been subdivided into three

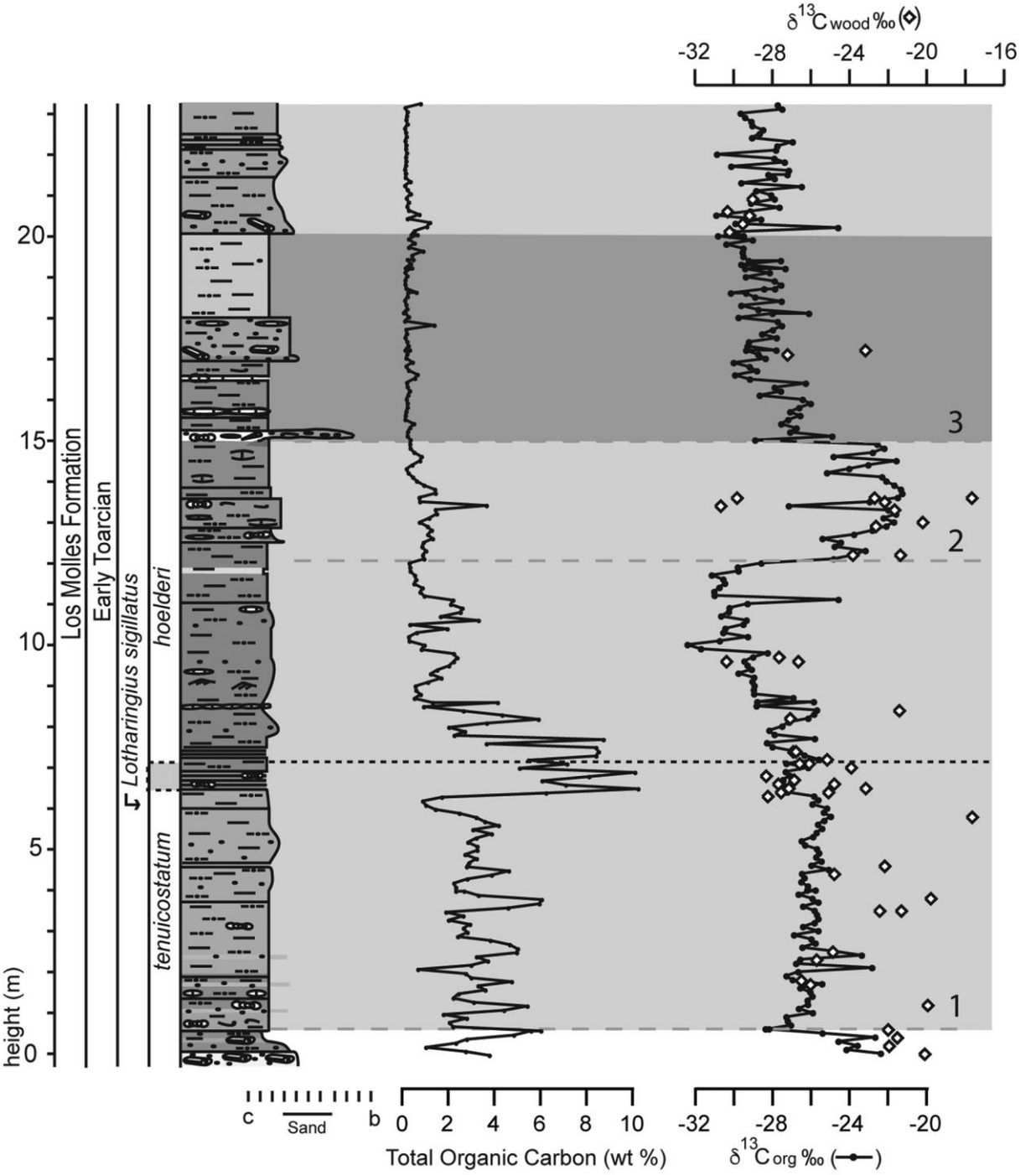

Figure 7. Section at Arroyo Lapa South, showing $\delta^{13}C_{org}$ from bulk sediment and wood (diamonds) and total organic carbon (TOC) profile. The short-dashed black line indicates the location of the refined zonal boundary between the *tenuicostatum* and *hoelderi* ammonite zones. The lighter shaded box indicates the Toarcian oceanic anoxic event and associated carbon isotope excursion, followed by a return to isotopically lighter values (darker shaded box). Note the increase in the TOC (from ~2% to ~11%) leading to the top of the *tenuicostatum* zone, with relatively high values persisting into the *hoelderi* zone, as well as the negative 6‰–7‰ excursion in the $\delta^{13}C_{org}$ from both bulk sediment and wood following the *tenuicostatum-hoelderi* boundary; also note the 8‰–10‰ positive excursion (~12–15 m, above level 2). Level 3 indicates an erosional surface that truncates this part of the section and is followed by a return to more isotopically light values. The gray long-dashed lines and labels 1 and 3 are also referred to in the text. The column on the left-hand side of the figure indicates lithostratigraphy, stage, lowest nannofossil occurrence, Andean ammonite zone, and the simplified graphical log. Detailed key of lithologies and other key elements are given in figure 8. A color version of this figure is available online.

informal intervals, as defined by Gulisano and Gutiérrez Pleimling (1995*b*, p. 61). These intervals are thought to represent fine-grained outer shelf (interval I) and basinal shale and turbidite deposits (intervals II and III; Gulisano and Gutiérrez Pleimling 1995*b*; Valencio et al. 2005). The Arroyo Serrucho stratigraphy reported on here comprises three distinct sections (fig. 4): A–A′ (~49 m), B–B′ (~14 m) and C–C′ (~28 m; fig. S3; figs. S1–S3 are available online).

Section A–A′ is ~49 m thick and represents Tres Esquinas Formation interval I sediments. The A–A′ section comprises medium-gray mudstone with thin, interbedded, buff-colored, very fine-grained sandstone beds, with some laminated dark-gray and brown shale. Siderite-cemented concretions, sandstone, and mudstone beds are common throughout the section from ~13 to 27.5 m. Fossiliferous limestone beds occur from 31 to 37.2 m, as well as at the top of the section at 48 m, indicating the boundary between intervals I and II of the Tres Esquinas Formation. Ammonite zones from this section begin with the early Toarcian *tenuicostatum* zone, which is marked by the LwO of *Dactylioceras* (*Orthodactylites*) cf. *anguinum* (Reinecke) (cf. von Hillebrandt 2006, p. 34, 263; von Hillebrandt and Schmidt-Effing 1981; Riccardi et al. 2011) collected ex situ from 1 m below the base of the section. The base of the *hoelderi* zone is marked by the LwO of *Harpoceras* cf. *serpentinum* (Schlotheim) (LwO 18.0 m). A significant number of bivalves were collected from section A–A′, two of which have ranges limited to the latest Pliensbachian to earliest Toarcian, *Terquemia andina* Damborenea (LwO 27.5 m) and *Entolium mapuche* Damborenea (LwO 37.1 m), while *Parvamussium pumilum* (Lamarck) (LwO 31.3 m) is limited to the Toarcian (Damborenea 2002). The rhynchonellid brachiopod *Rhynchonelloidea lamberti* Manceñido (LwO 37.1 m) is likewise confined to the early (but not earliest) Toarcian (Manceñido 1990).

Section B–B′ is located about 500 m south of A–A′ (fig. 4), with ~14 m of exposed succession. The lowermost part of the exposure comprises siltstone with interbedded limestone beds, <10 cm thick, indicative of Tres Esquinas Formation interval I. Ammonites, bivalves, and fossil wood are common in this part of the section. Above this is a gray mudstone with thin interbeds of siderite-cemented shale. The uppermost part of the section (8.3–14 m) comprises shale and laminated paper shale, with some fossiliferous mudstone and limestone. Ammonites from this section are indicative of the *hoelderi* zone, as evidenced by the presence of *Hildaites* cf. *murleyi* (Moxon) (cf. von Hillebrandt 1987; Howarth 1992, p. 168; Riccardi et al. 2011) and *Harpoceras* cf. *serpentinum* (Rein.) (cf. von Hillebrandt 1987; Howarth 1992, p. 109) at 9.5 and 11.1 m, respectively.

The third section, C–C′, located some 300 m northeast of section B–B′ (fig. 4), is ~28 m thick and represents sediments of the Toarcian Tres Esquinas Formation intervals I and II. The section continues upward into interval III. The lowermost unit (<4.5 m) comprises greenish-gray siltstone interbedded with fossiliferous limestone, whereas the upper unit (4.5–29 m; fig. S3) comprises dark-gray paper shale and calcareous mudstone, with 5–10-cm-thick gray fossiliferous limestone beds and thin interbedded tuffaceous units toward the top. Section C–C′ corresponds to the lowest ~28 m of the section described by Mazzini et al. (2010). These authors interpreted the lowest part of the section to include the boundary between the Pliensbachian Puesto Araya Formation and the Toarcian Tres Esquinas Formation, but no ammonites indicative of the Pliensbachian stage have been found at this locality. Importantly, what these authors mistook as the boundary at section C–C′ comprises a 45-cm-thick limestone containing two levels characterized by concentrations of bivalve shells, phosphatized ammonite steinkerns, and fossil wood (fig. 4*C*). These beds have the attributes of extreme condensation or hiatus of the *largaense* to *pacificum* zones (equivalent to the northwestern European *bifrons* zone). Biostratigraphic determination of the fossils from the Arroyo Serrucho sections confirms the presence of early and middle Toarcian strata.

Section C–C′ yields ammonites from the *hoelderi* zone, specifically the occurrence of *H.* cf. *murleyi* (Moxon) and *Cleviceras* cf. *chrysanthemum* (Yok.) at ~3.97 m. The presence of *H.* cf. *falciferum* (J. Sow.) and *Peronoceras* sp. (LwO 5.8 m) indicates the *hoelderi-largaense* zones. *Peronoceras* sp. and *Harpoceras* cf. *subplanatum* (Oppel) (LwO 6.4 m) indicate the presence of the *pacificum* zone. The occurrence of *Collina chilensis* (Hill. & Sch.-Effing) and *H.* cf. *subplanatum* (Oppel) at 13.07 m is indicative of the mostly middle Toarcian *C. chilensis* assemblage zone, which is equivalent to the northwestern European uppermost *bifrons* and *variabilis* zones (fig. 5). Ammonites indicative of the *Phymatoceras* assemblage zone (≈*thouarsense* standard zone, late Toarcian) occur at 26.7 m.

Tres Esquinas Formation interval I in the Serrucho area represents sediments deposited in an outer-shelf environment, with some storm deposits and normal marine faunas. Intervals II and III represent a deeper-water setting, with finer grained sediments and an increase in the abundance of turbidites in interval III (Gulisano and Gutiérrez Pleimling 1995*b*, p. 61).

Carbon-Isotope Stratigraphy and Organic-Matter Content

At Arroyo Lapa North (fig. 6), a minor negative CIE with values as low as −30.8‰ occurs at 1.4–2.4 m (level A in fig. 6), within a zone of biostratigraphic uncertainty and a concurrent 1%–2% increase in TOC. This excursion may represent a feature similar to that documented in Pliensbachian-Toarcian boundary sections from several locations in northwestern Europe (cf. Hesselbo et al. 2007; Littler et al. 2010). However, some biostratigraphic uncertainty exists (below 14.5 m) for this interval in Arroyo Lapa North, hindering the accurate determination of the stage boundary.

Above the exposure gap (>8.1 m), the majority of samples have $\delta^{13}C_{org}$ values of <−30‰, and values as low as about −32‰ are also present (14.5 and 18.7–19.9 m). An abrupt positive excursion to heavier values (>−24‰) is recorded from 16.3 to 17.4 m, and additionally, a positive shift occurs above 27 m at the top of the section, with values heavier than −26‰ recorded in bulk sediment (above line C in fig. 6). Isotopic values of fossil wood are relatively light through the section, <−26‰, with values as low as −30.7‰ (8.4 and 24.2 m), although values become heavier (about −24‰) at the top of the section.

The TOC values in this section are relatively low, remaining below ~1% in the lowest ~14 m and increasing in the top ~8 m (fig. 6). There is a slight increase in TOC at 14.5 m, with values reaching ~2.4% (14.9 m), and two additional increases in TOC, with values of ~2% at 17.9 m and ~2.3% at 19.5 m. These higher values correspond to the most isotopically light values of $\delta^{13}C_{org}$ (<−30‰) and are followed by a return to relatively low TOC values, <1%. Above 24 m (above level C), there is a gradual increase in TOC, with values as high as ~6% (26.6 and 26.8 m), which is coincident with the presence of abundant charcoalified wood fragments in the sandstone beds. HI data from 2 to 20 m give values ranging from 12 to 94 mg HC/g TOC, indicating the presence of mostly terrestrial organic matter in this part of the section and/or differing degrees of oxidative degradation of such material. HI data at 24 m give a value of 293 mg HC/g TOC, reflecting type II organic matter with a clear marine component (Tissot et al. 1974; Pasley et al. 1991). The T_{max} values range from 430° to 444°C, suggesting that the organic matter is largely immature or marginally mature.

At Arroyo Lapa South (fig. 7), there is a negative shift to $\delta^{13}C_{org}$ of −28.3‰ at 0.5 m (level 1 in fig. 7); following this, there is a return to more isotopically heavy values of about −25‰, between 0.5 and 5 m. Above 5 m, there is a stepped negative CIE, with $\delta^{13}C_{org}$ values decreasing from −28‰ to a minimum of about −32.5‰ at a level ~3 m above the *tenuicostatum-hoelderi* ammonite zonal boundary (i.e., at the 10-m height). Values of $\delta^{13}C_{org}$ in Arroyo Lapa South stay below −28‰ through the lower half of the *hoelderi* ammonite zone, with a positive excursion over the interval 12.1–14.9 m, with values as high as −21.4‰, followed by a return to isotopically lighter values of <−26‰. Although it was suggested in Al-Suwaidi (2010) that this positive excursion lay above an erosion surface (level 2 in fig. 7) and represented material reworked in a slump, more-detailed examination of the succession in the field has failed to find supporting evidence for either the erosion surface or slump. A negative shift back to $\delta^{13}C_{org}$ values between about −27‰ and −30‰ occurs coincidently with the level of fossil-rich conglomerate and demonstrable erosion surface, at the ~15-m (level 3 in fig. 7); a subsequent shift to lighter values of <−29‰ shows a stepped trend. The $\delta^{13}C_{wood}$ record also shows a 6‰ negative excursion leading up to the *tenuicostatum-hoelderi* ammonite zonal boundary, with values falling to about −30.7‰ at the 13.4-m height.

The TOC weight percentages show an increase from ~4% to 10.3% at 6.5 m, followed by a stepped decrease above the *tenuicostatum-hoelderi* ammonite zonal boundary back to <3%. HI data give values ranging from 49 to 425 mg HC/g TOC, indicating the presence of a mixture of terrestrial and marine organic matter throughout the section (type II) and/or differing degrees of oxidative degradation of such material (fig. S2). However, that part of the section with relatively high TOC (>4%) also has a relatively high HI (390–425 mg HC/mg TOC), indicating an appreciable component of marine organic matter in the sediment in this interval (6.5–7.5 m). The T_{max} values are very similar to those in Arroyo Lapa North, and values range from 430° to 438°C, indicating that the organic matter is thermally immature or marginally mature.

At Arroyo Serrucho, in the lower part of section A–A′ (fig. 8), $\delta^{13}C_{org}$ values fall to −31.1‰ at ~3 m above the *tenuicostatum-hoelderi* ammonite zone boundary (~19.5 m); this point coincides with a minor relative enrichment in organic matter (1.2% TOC, 22.5 m). The $\delta^{13}C_{org}$ values in A–A′ become isotopically heavier upward, with an abrupt positive step at ~32 m, where $\delta^{13}C_{org}$ values increase to −23‰. The TOC content in this section is relatively low throughout, <0.5% in most samples, but values increase toward the *tenuicostatum-hoelderi* ammonite zone boundary and remain higher, >0.5%, through the lower part of the *hoelderi* zone.

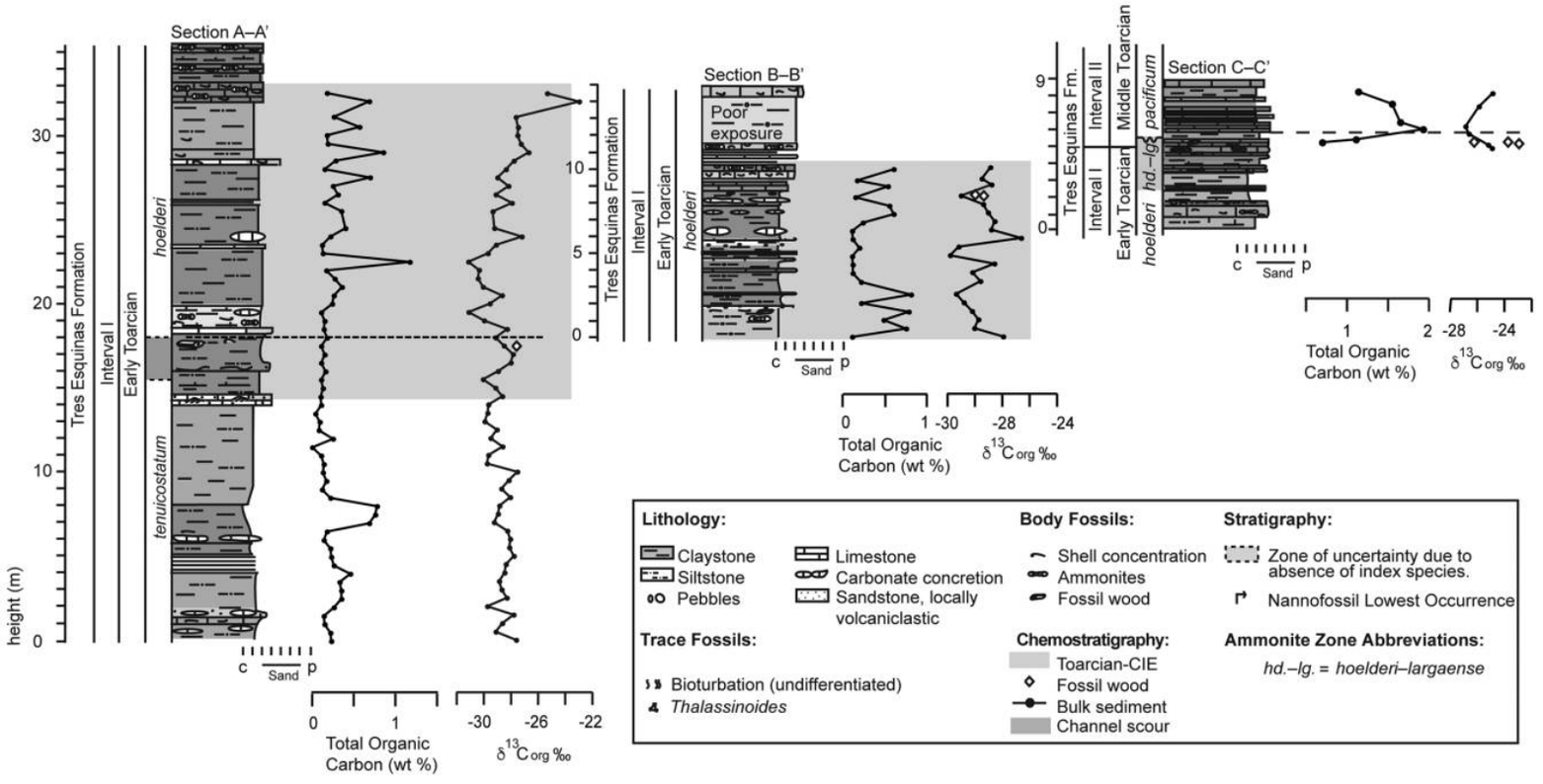

Figure 8. Three sections at Arroyo Serrucho, showing $\delta^{13}C_{org}$ from bulk sediment (black dots) and wood (diamonds) and total organic carbon (TOC) profile. Dashed lines indicate the location of ammonite zonal boundaries. The shaded box indicates location of the Toarcian oceanic anoxic event and associated carbon isotope excursion (CIE). Note that the TOC wt% is very low in all sections but that in the A–A′ section it increases upward following the *tenuicostatum-hoelderi* ammonite zonal boundary. Also note the negative excursion in $\delta^{13}C_{org}$ of −4‰ in bulk sediment at the *tenuicostatum-hoelderi* ammonite zone boundary. Section B–B′ also shows isotopically light values of <−28‰ through the section and likely corresponds to the lowermost *hoelderi* zone. Section C–C′ indicates a hiatus or condensation in the *hoelderi-largaense* zone. The $\delta^{13}C_{org}$ values in this section are generally isotopically heavier than those in sections A and B. The column on the left-hand side of each panel indicates lithostratigraphy, stage, Andean ammonite zone, and the simplified graphical log. A detailed key of lithologies and other key elements related to the logs and chemostratigraphy are given in the bottom right-hand corner of the image. A color version of this figure is available online.

Section B–B′ at Arroyo Serrucho, which comprises strata assigned to the *hoelderi* zone, shows $\delta^{13}C_{org}$ values that are isotopically relatively light, <−29‰ and as low as −31.8‰ at 4.78 m, followed by an abrupt shift to more positive values of −26.6‰ at 5.78 m and a second negative shift to values <−29‰ through the remainder of the section. The TOC is also relatively low through this section, with most values < 0.5%, although there is a slight increase to 0.8% at 2.5 m, coincident with $\delta^{13}C_{org}$ values of −31.3‰. On the basis of values in section B–B′, the strata appear to correspond to the negative CIEs immediately following the *tenuicostatum-hoelderi* zonal boundary in section A–A′ (fig. 8). Fossil wood samples from the upper part of this section are also isotopically relatively light, with values of −28‰.

Section C–C′ at Arroyo Serrucho, which comprises sediments of the *hoelderi* to *chilensis* zones, shows $\delta^{13}C_{org}$ values ranging from −24‰ to −26.8‰ and fossil wood samples with $\delta^{13}C$ values ranging from −22.7‰ to −25.1‰. There is relative enrichment in TOC in this section, with values in the range 0.8%–1.9% through the section, in contrast to sections A–A′ and B–B′.

Arroyo Serrucho and the Age of the T-OAE

A composite profile combining the new $\delta^{13}C_{org}$ data and biostratigraphy from Arroyo Serrucho, together with the $\delta^{13}C_{org}$ data of Mazzini et al. (2010), is shown in figure 9*B*. This synthesis is based on the combination of ammonite biostratigraphy, $\delta^{13}C_{org}$ stratigraphy, and field relations (fig. 4). Given the lithostratigraphic and ammonite evidence presented above, it is clear that the section sampled by Mazzini et al. (2010) and the C–C′ section at Arroyo Serrucho from this study are for the most part higher (and younger) than the section sampled at A–A′ and B–B′. In Mazzini et al. (2010), the location of the *tenuicostatum-hoelderi* ammonite zonal boundary was inferred from the presence of the bivalve *Bositra*, which has a long range, extending from the Pliensbachian to the Callovian in Andean areas (Damborenea 1987*b*), and may reach an even younger age elsewhere (Jefferies and Minton 1965; Ros Franch et al. 2014); consequently, it is not a particularly useful biostratigraphic marker in the Southern Hemisphere. Moreover, here it has been recorded throughout the *Collina chilensis* zone, reaching the *Phymatoceras* assemblage zone.

Mazzini et al. (2010) also report the ammonite *Hildaites* cf. *murleyi* (Moxon) from the uppermost part of their section (64 m; fig. 9*A*); this taxon is considered indicative of the Andean *hoelderi* zone (Riccardi 2008*a*, 2008*b*). However, the occurrence of this taxon so high in the section is incompatible with the presence of ammonites of the *pacificum* and *chilensis* zones, equivalent to the northwestern European upper *bifrons* to *variabilis* zone, ~60 m lower in the section (fig. 9*A*), as recorded here.

The $\delta^{13}C_{org}$ data of Mazzini et al. (2010) are also incompatible with identification of the T-OAE stratigraphically higher than section C–C′ in the Tres Esquinas Formation at Arroyo Serrucho; the minimum recorded $\delta^{13}C_{org}$ values of −29.8‰ at this level are not typical of the minimum $\delta^{13}C_{org}$ values for the T-OAE in Argentina in Arroyo Lapa or Arroyo Serrucho, which are consistently lower than −30‰. Similarly, $\delta^{13}C_{org}$ values for well-documented T-OAE shales in Europe and North America are consistently less than −30‰ (e.g., Jenkyns and Clayton 1986, 1997; Schouten et al. 2000; Jenkyns et al. 2001, 2002; Schmid-Röhl et al. 2002; Kemp et al. 2005; Sabatino et al. 2009; Caruthers et al. 2011; Gröcke et al. 2011; Kafousia et al. 2011; Hermoso et al. 2012). Although data from Japan show values only as low as −28.5‰ for the Toarcian, the main source of organic matter in this section is terrestrial, which typically has heavier $\delta^{13}C_{org}$ values than marine organic matter (Kemp and Izumi 2014).

Mazzini et al. (2010) assigned the T-OAE an age of 182.16 ± 0.6 Ma (onset) to 180.16 ± 0.66 Ma (recovery), on the basis of calculations assuming constant sedimentation rates and the supposition that ashes yielding dates of 181.42 ± 0.24 and 180.59 ± 0.43 Ma were from the level of the T-OAE. Given our ammonite biostratigraphy, carbon isotope data, and field examination of the section examined by Mazzini et al. (2010), it is unlikely that the section records a constant sedimentation rate or that these ages are coincident with the T-OAE. Sell et al. (2014) also examined a Toarcian section in Palquilla, Peru, and dated several ash beds through the section, coupling these radiometric ages with the high-resolution biostratigraphy of Guex et al. (2012). Their dates of 181.99 ± 0.13 and 182.128 ± 0.081 Ma fall in the middle Toarcian *bifrons* zone, and a stratigraphically higher ash was dated at 180.35 ± 0.39 Ma, belonging to the biostratigraphically determined latest Toarcian (fig. 10). In addition, Riccardi and Kamo (2012, 2014) also radiometrically dated an ash bed from the latest Pliensbachian to earliest Toarcian *tenuicostatum* zone at Chacay Melehue, Argentina, and assigned it a weighted mean age of 183.16 ± 0.11 Ma. These studies further support the interpretation that the absolute age data used by Mazzini et al. (2010) to determine the age of the T-OAE/CIE actually record a time interval that postdates the event. The new work of Burgess et al. (2015), coupled

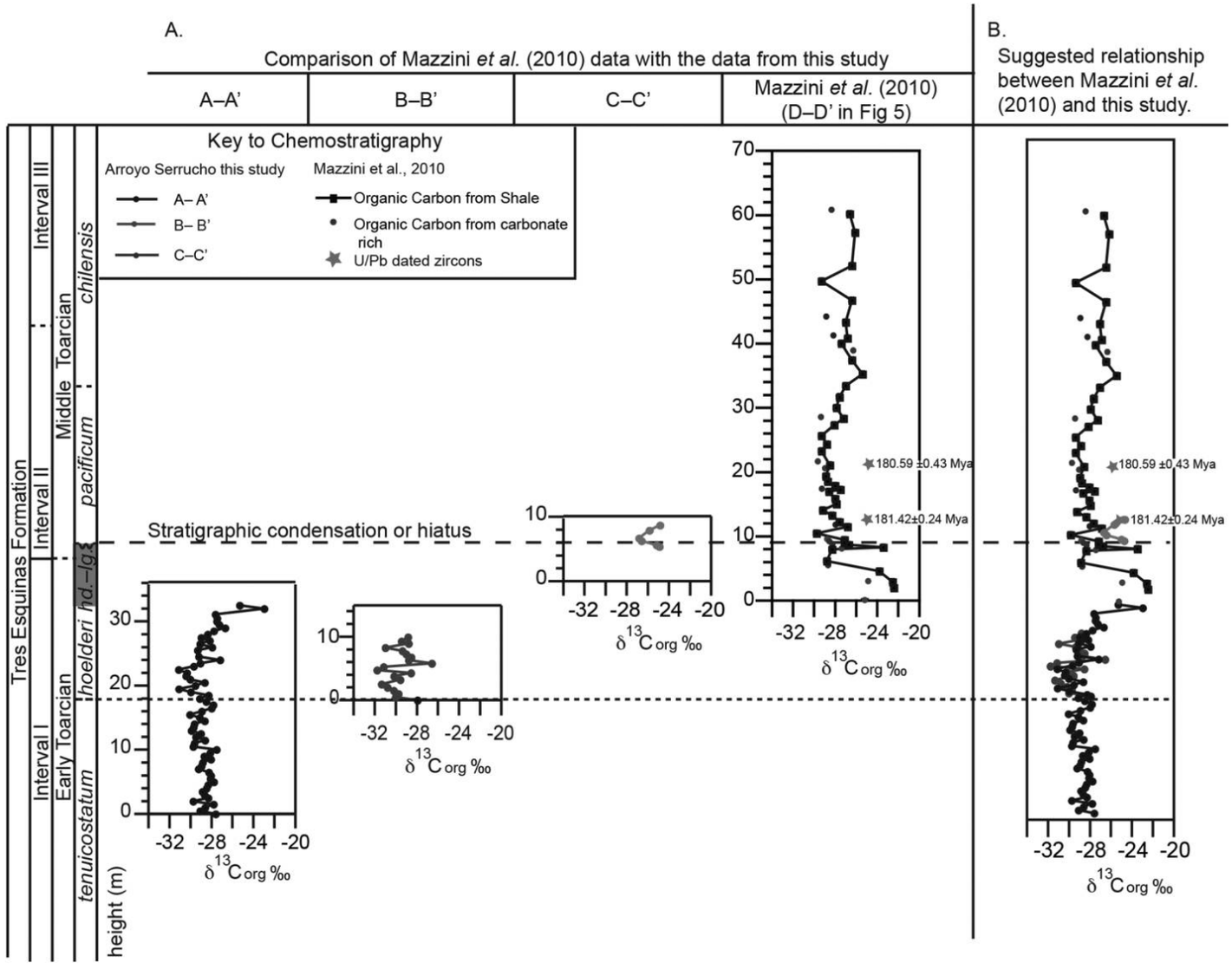

Figure 9. *A*, Comparison of $\delta^{13}C_{org}$ and age data from the Mazzini et al. (2010) study of Arroyo Serrucho and data from this study. The Mazzini et al. (2010) data are not correlative with the data in this study from the *tenuicostatum-hoelderi* ammonite zone boundary, but, from field evidence, their section lies stratigraphically above A–A′ and B–B′ and corresponds to the upper part of section A–A′ and section C–C′; *hd.-lg* = *hoelderi-largaense* zone. *B*, Possible relationship between the Mazzini et al. (2010) section and the sections in this study from Arroyo Serrucho, based on field observations of the area and $\delta^{13}C_{org}$ correlation. Also note the location of the dated ashes with respect to the chemostratigraphy and high-resolution biostratigraphy from this study. As these ashes occur in the *pacificum* and/or *chilensis* zone (equivalent to the *bifrons* to *variabilis* zones), they are not useful in constraining the age of the base of the Toarcian. The short-dashed line indicates the location of the *tenuicostatum-hoelderi* ammonite zone boundary, whereas the long-dashed line indicates the level of stratigraphic condensation or hiatus in the record, which truncates or condenses the *hoelderi-largaense* ammonite zone and is followed by sediments containing ammonites from the *pacificum* and *chilensis* ammonite zones. A color version of this figure is available online.

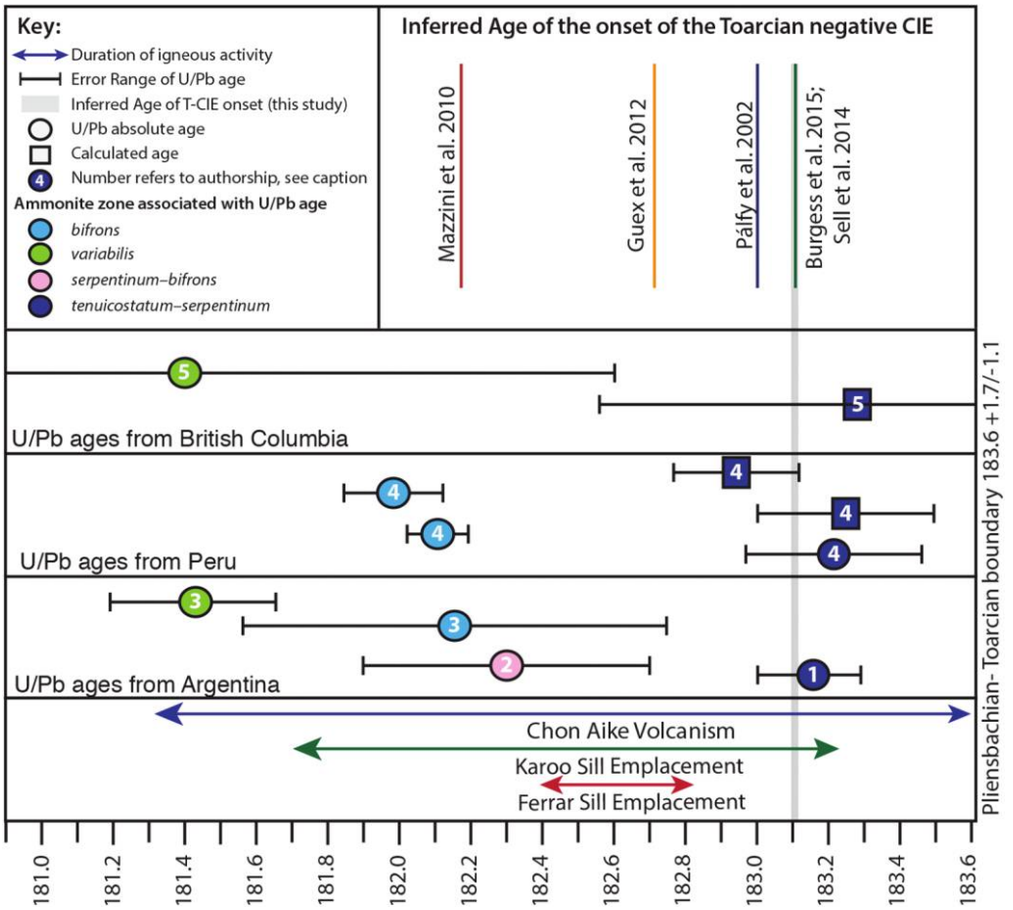

Figure 10. Comparison of estimated timing of Karoo-Ferrar sill emplacement (Svensen et al. 2007, 2012; Burgess et al. 2015) and Chon Aike volcanism (Feraud et al. 1999), with radiometric ages from ashes associated with Early Toarcian ammonite zones from Argentina (1: Riccardi and Kamo 2014; 2: Leanza et al. 2013; 3: Mazzini et al. 2010), Peru (4: Sell et al. 2014), and British Columbia (5: Pálfy et al. 2002) and estimated ages assigned to the onset of the negative excursion of the Toarcian oceanic anoxic event. The age of the Pliensbachian-Toarcian boundary is assigned as $183.6^{+1.7}_{-1.1}$ from Pálfy et al. (2002). Details of radiometric ages can be found in tables S1 and S2 (available online). T-CIE = Toarcian carbon isotope excursion.

with the existing radiometric ages from Pálfy et al. (2002), Sell et al. (2014), and Riccardi and Kamo (2012, 2014) and placing the Mazzini et al. (2010) and Leanza et al. (2013) dates in the correct biostratigraphic context (fig. 10), indicates that the onset of the Toarcian CIE was about 183.1 Ma, coincident with Karoo sill emplacement, in agreement with Burgess et al. (2015) and Sell et al. (2014).

From our compilation (fig. 10) of the radiometric ages associated with Karoo-Ferrar LIP activity and the various biostratigraphically relevant intervals, the most negative values associated with the Toarcian CIE coincide with the onset of Ferrar sill emplacement, as well as Karoo sill emplacement, at 182.8 Ma. It also appears that the Pliensbachian-Toarcian negative excursion likewise coincides with onset of Chon Aike volcanism.

The T-OAE in the Neuquén Basin

Correlation between the three sections in the Neuquén Basin, Argentina, can be made on the basis of ammonite biostratigraphy and carbon isotope stratigraphy (fig. 11). The Arroyo Lapa North section shows evidence of two major negative CIEs with values below −31‰ (correlation lines b and c in fig. 11), interrupted by a positive isotope excursion with values reaching −24‰ (fig. 11). This second, or stratigraphically higher, negative isotope excursion (fig. 11) is followed by a gradual positive

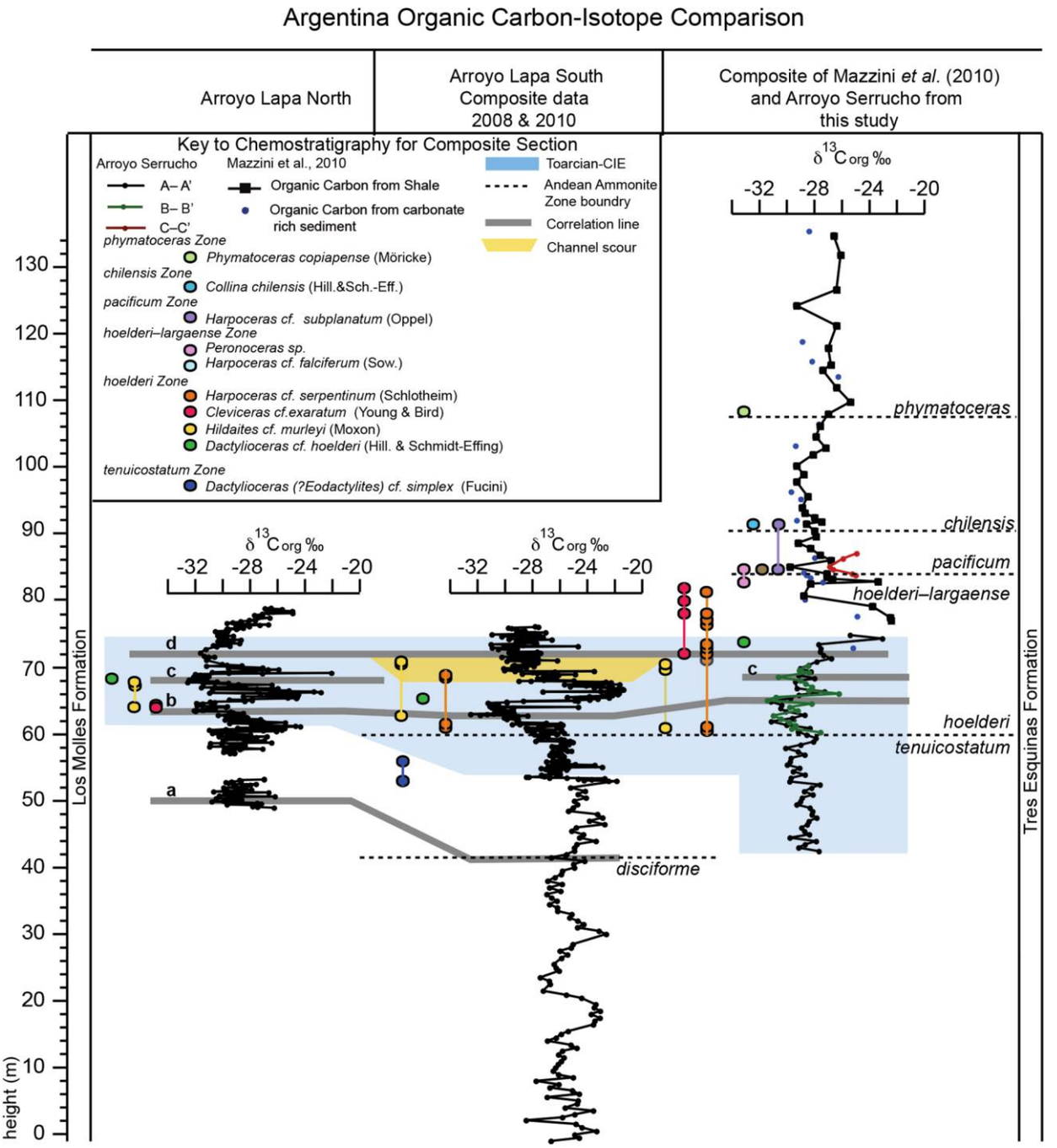

Figure 11. Comparison of $\delta^{13}C_{org}$ data from Arroyo Lapa North and South and the possible relationship between the Mazzini et al. (2010) section and the sections in this study from Arroyo Serrucho. Indicated are the occurrence and range within the section of key ammonites (colored circles). Also indicated is the possible location of the Pliensbachian-Toarcian boundary (level a), the two negative carbon isotope excursions (CIEs; levels b and c), and the possible correlation of the top of the sections (level d). Also note that these two negative excursions (levels b and c) in Arroyo Lapa North are separated by an abrupt transition to isotopically heavy $\delta^{13}C_{org}$, with values of $>-22‰$, exceptionally heavy compared to the background $\delta^{13}C_{org}$ values from Arroyo Lapa South and Arroyo Serrucho of about $-26‰$. The column on the left-hand side of the figure indicates the lithostratigraphy for Arroyo Lapa North and South. The column on the right-hand side of the figure indicates the lithostratigraphy for Arroyo Serrucho. Note that ammonite zonation section is approximated on the basis of the composite section. Dashed lines indicate the location of ammonite zone boundaries. The light-blue box highlights the main body of the Toarcian carbon isotope excursion in all three sections.

recovery and return to values of >−28‰. The Arroyo Lapa North section lacks the conglomerate (and presumably the submarine fan-channel thalweg) that characterizes Arroyo Lapa South; we hence interpret the North section to be a more complete record of events during the early Toarcian *tenuicostatum-hoelderi* (~*tenuicostatum-serpentinum*) zones. These negative CIEs and the intervening positive excursions may represent exaggerations of the steps recorded in European sections of the same age (e.g., Kemp et al. 2005; Hesselbo et al. 2007; Hesselbo and Pieńkowski 2011; Hermoso et al. 2012), or they may record events that occurred after the early T-OAE (e.g., line d in fig. 11).

The Arroyo Lapa South section records the initial negative CIE of the T-OAE and the abrupt positive recovery, which is correlative with Arroyo Lapa North and Arroyo Serrucho (level b in fig. 11), but the second, stratigraphically higher negative isotope excursion, as recorded in Arroyo Lapa North and Arroyo Serrucho (level c in fig. 11), is apparently cut out in the South section by the submarine channel. The strata above the fossil-rich conglomerate show a return to isotopically light values of about −29‰ and likely record rapid channel infill. The upper part of this section (>74 m in fig. 11; >19 m in fig. 7) may be equivalent to quantitatively similar light isotopic values recorded above level d (fig. 11) in the Arroyo Lapa North (>22 m; fig. 6) and Arroyo Serrucho (>31 m; fig. 8) sections.

At Arroyo Serrucho, the initial large negative CIE of the T-OAE is recorded in the Tres Esquinas Formation interval I. Interval II of the Tres Esquinas records the positive recovery, but again the section is truncated or very strongly condensed in the *hoelderi-largaense* zone, in this case at a level (~6 m in C–C′; fig. 8) represented by the phosphatic-nodule beds (fig. 4*C*). Above this interval lie deeper-water shale and turbidite deposits of the Tres Esquinas Formation intervals II and III (Gulisano and Gutiérrez-Pleimling 1995*b*, p. 61) and the correlative section described by Mazzini et al. (2010).

Major sea level rises in the early/middle Toarcian have been inferred from other localities in the Neuquén Basin (Legarreta and Uliana 1996; Burgess et al. 2000; Lanés 2005) as well as from Northern Hemisphere locations such as in sections from Spain, Portugal, and the United Kingdom (e.g., Hesselbo and Jenkyns 1998; Duarte 2007; Gómez et al. 2008; Hesselbo 2008). Hallam (1981, 1988) interpreted this phenomenon as a eustatic sea level rise. It is possible that, as a result of this sea level rise in the early Toarcian, many sections globally are condensed or show a hiatus during the interval where the second negative CIE is recorded in Arroyo Lapa North (level c in fig. 11). Further work in the Southern Hemisphere and closer scrutiny of data from the Northern Hemisphere are necessary to determine whether this sea level rise had a global impact on the preservation of carbon isotope signatures recorded from Toarcian sediments or whether these chemostratigraphic signatures in the Neuquén Basin are simply a result of local sedimentary variability.

The second, stratigraphically higher negative isotope excursion (level c in fig. 11) in the Neuquén Basin may also offer new insight into the global impact of the Karoo-Ferrar and Chon Aike LIPs. A study of marine extinction events in the northern part of Panthalassa in the Early Jurassic shows evidence for multiple extinctions recorded by loss of species diversity in ammonites and foraminifers, which can be correlated with episodic LIP activity in the Karoo Basin (Caruthers et al. 2013). Correlation of species diversity data with calibrated ages from Pálfy and Smith (2000) and Gradstein et al. (2012), set against known eruptive ages from the Karoo LIP (Jourdan et al. 2008), suggests at least four significant extinction events from the Toarcian that can be correlated with LIP activity, only one of which corresponds to the T-OAE (Caruthers et al. 2013). In addition, new astrochronological work from Japan by Ikeda and Hori (2014) also suggests two discrete events in the early Toarcian, possibly linked to two large magmatic pulses from Karoo. New radiometric ages indicate that the LIP activity in Karoo began about 183.2 Ma and lasted about 1 m.yr. (Svensen et al. 2012; Burgess et al. 2015), with Ferrar sill emplacement occurring between ~182.8 and 182.3 Ma (Burgess et al. 2015; fig. 10). Karoo magmatic activity, specifically the intrusive events, has commonly been associated with the T-OAE because these events potentially have expelled volatiles from intrusion into organic-rich country rock, indicating that the T-OAE likely has an age of 183.1 Ma (Sell et al. 2014; Burgess et al. 2015). Dike intrusions into organic-rich shale in Ferrar after the initial Karoo intrusions could explain the stepped nature of the Toarcian negative CIE, as seen in both Arroyo Lapa North and in Arroyo Serrucho, especially given that, in both Karoo and Ferrar, dike intrusion was not continuous but appears to have occurred periodically (Burgess et al. 2015).

It is also possible that the positive excursion marking the end of the main negative CIE in Arroyo Lapa and Arroyo Serrucho is indicative of a temporary period of volcanic quiescence, during which time a large amount of organic matter (isotopically light) was drawn down into the global oceans to dominate the global carbon isotope signal. Percival et al. (2015) have also demonstrated a clear link be-

tween activity at Karoo-Ferrar and the Pliensbachian-Toarcian boundary event and T-OAE, using mercury/TOC as an indicator of enhanced atmospheric Hg availability, sourced from volcanism. Additional work is needed to understand the total extent and impact of these volcanic provinces on the ocean-atmosphere system, and it may be necessary to give special consideration to silicic volcanism in terms of its impact on marine algal productivity (Self 2006), especially given that the Chon Aike silicic volcanic province erupted over a time interval similar to that of the main activity at Karoo-Ferrar (186–181.3 Ma; Feraud et al. 1999) and that the estimated extent of Chon Aike is at least 235,000 km^3, which places it among the largest known silicic LIPs (Pankhurst et al. 1998; Bryan et al. 2010).

Conclusion

At two locations, in the southeast (Arroyo Lapa) and the northeast (Arroyo Serrucho) of the Neuquén Basin, Argentina, sections dated biostratigraphically to the *tenuicostatum-hoelderi* zones show $\delta^{13}C_{org}$ values below −30‰ and a relative increase in TOC, both characteristic geochemical signatures of the T-OAE. A complex sequence comprising three negative CIEs is recorded in the Arroyo Lapa North section, with two large intervening positive isotope excursions with values as positive as about −24‰. Whether these positive excursions have a global or local expression is currently unknown. In Arroyo Lapa South, the first, or stratigraphically lowest, negative isotope excursion is recorded, as is the very abrupt positive excursion following this event, but the upper part of the section is eroded beneath a channel. The $\delta^{13}C_{org}$ values of the channel fill are relatively isotopically light (<−30‰) and may be equivalent to the third negative isotope excursion recorded in Arroyo Lapa North.

New data from Arroyo Serrucho indicate a negative CIE but do not capture events with the same structure as observed at Arroyo Lapa North. Field observations and biostratigraphic examination of the section described by Mazzini et al. (2010) suggest that the radiometric ages and chemostratigraphy generated by these authors occur in the Toarcian *pacificum* and/or *chilensis* zone, equivalent to the *bifrons* to *variabilis* zone from Europe, and are too young, by more than 1 m.yr., to represent the Toarcian negative CIE. The onset of the Toarcian negative CIE, based on the radiometric ages from Burgess et al. (2015) and Sell et al. (2014), is likely 183.1 Ma, coincident with the onset of Karoo sill emplacement. Elevated levels of mercury, of likely volcanic origin, which have been found in the Arroyo Lapa South section and other Toarcian localities in northern Europe, suggest a connection between large-scale volcanism and expulsion of globally distributed volatiles, in the cases of both the Pliensbachian-Toarcian boundary carbon isotope event and the T-OAE (Percival et al. 2015), and further support the strong link between eruptive and intrusive phases of Karoo-Ferrar and Chon Aike volcanism.

The records from Arroyo Serrucho and Arroyo Lapa South demonstrate well the potential complexity created by variation in depositional settings within a basin and highlight the value of detailed lithostratigraphic work in establishing a complete and typical record of carbon isotope variations through an event of major environmental change. The new high-resolution data set from Arroyo Lapa North is at present the most completely documented record of the T-OAE from the Southern Hemisphere. The data unambiguously illustrate the global reach of the T-OAE.

ACKNOWLEDGMENTS

We thank the Petroleum Institute, University and Research Centre and the Scholarship Coordination Office, Abu Dhabi, United Arab Emirates; the Geological Society, London; the Jeremy Wilson Foundation; the Consejo Nacional de Investigaciones Científicas y Técnicas (CONICET, Argentina); and the American Association of Petroleum Geologists for financial support.

REFERENCES CITED

Al-Suwaidi, A. H.; Angelozzi, G. N.; Baudin, F.; Damborenea, S. E.; Hesselbo, S. P.; Jenkyns, H. C.; Manceñido, M. O.; and Riccardi, A. C. 2010. First record of the early Toarcian oceanic anoxic event from the Southern Hemisphere, Neuquén Basin, Argentina. J. Geol. Soc. Lond. 167:633–636.

Beerling, D. J.; Lomas, M. R.; and Gröcke, D. R. 2002. On the nature of methane gas-hydrate dissociation during the Toarcian and Aptian oceanic anoxic events. Am. J. Sci. 302:28–49.

Blakey, R. 2007. Early Jurassic rectangular paleogeographic map in Mollwide. http://jan.ucc.nau.edu/~rcb7/200marect.jpg. Accessed November 2009.

Bodin, S.; Mattioli, E.; Fröhlich, S.; Marshall, J. D.; Boutib, L.; Lahsini, S.; and Redfern, J. 2010. Toarcian carbon isotope shifts and nutrient changes from the northern

margin of Gondwana (High Atlas, Morocco, Jurassic): palaeoenvironmental implications. Palaeogeogr. Palaeoclimatol. Palaeoecol. 297:377–390.
Bouma, A. H. 2000. Coarse-grained and fine-grained turbidite systems as end member models: applicability and dangers. Mar. Pet. Geol. 17:137–143.
Bryan, S. E.; Ukstins Peate, I.; Peate, D. W.; Self, S.; Jerram, D. A.; Mawby, M. R.; Marsh, J. S.; and Miller, J. A. 2010. The largest volcanic eruptions on Earth. Earth-Sci. Rev. 102:207–229.
Burgess, P. M.; Flint, S.; and Johnson, S. 2000. Sequence stratigraphic interpretation of turbiditic strata: an example from Jurassic strata of the Neuquén Basin, Argentina. Geol. Soc. Am. Bull. 112:1650–1666.
Burgess, S. D.; Bowring, S. A.; Fleming, T. H.; and Elliot, D. H. 2015. High-precision geochronology links the Ferrar large igneous province with early-Jurassic ocean anoxia and biotic crisis. Earth Planet. Sci. Lett. 415:90–99.
Caminos, R.; Cingolani, C. A.; Hervé, F.; and Linares, E. 1982. Geochronology of the pre-Andean metamorphism and magmatism in the Andean Cordillera between latitudes 30° and 36°. Earth-Sci. Rev. 18:333–352.
Caruthers, A. H.; Gröcke, D. R.; and Smith, P. L. 2011. The significance of an Early Jurassic (Toarcian) carbon-isotope excursion in Haida Gwaii (Queen Charlotte Islands), British Columbia, Canada. Earth Planet. Sci. Lett. 307:19–26.
Caruthers, A. H.; Smith, P. L.; and Gröcke, D. R. 2013. The Pliensbachian-Toarcian (Early Jurassic) extinction, a global multi-phased event. Palaeogeogr. Palaeoclimatol. Palaeoecol. 386:104–118.
Coffin, M. F.; Duncan, R. A.; Eldholm, O.; Fitton, J. G.; Frey, F. A.; Larsen, H. C.; Mahoney, J. J.; Saunders, A. D.; Schlich, R.; and Wallace, P. J. 2006. Large igneous provinces and scientific ocean drilling: status quo and a look ahead. Oceanography 19(4):150–160.
Coira, B.; Davidson, J.; Mpodozis, C.; and Ramos, V. 1982. Tectonic and magmatic evolution of the Andes of northern Argentina and Chile. Earth-Sci. Rev. 18:303–332.
Damborenea, S. E. 1987*a*. Early Jurassic Bivalvia of Argentina. Part 1: stratigraphical introduction and superfamilies Nuculanacea, Arcacea, Mytilacea and Pinnacea. Palaeontogr. Abt. A 199:23–111.
———. 1987*b*. Early Jurassic Bivalvia of Argentina. Part 2: superfamilies Pteriacea, Buchiacea and part of Pectinacea. Palaeontogr. Abt. A 199:113–216.
———. 1989. El género *Posidonotis* Losacco (Bivalvia, Jurásico inferior): su distribución estratigráfica y paleogeográfica. *In* H. Leanza, org. Simposio invertebrados fósiles del Paleozoico y Mesozoico. IV Congreso Argentino de Paleontología y Bioestratigrafía (Mendoza, 1986), Actas 4:45–51.
———. 2002. Early Jurassic Bivalvia of Argentina. Part 3: superfamilies Monotoidea, Pectinoidea, Plicatuloidea and Dimyoidea. Palaeontogr. Abt. A 265:1–119.
Digregorio, R. E.; Gulisano, C. A.; Gutiérrez Pleimling, A. R.; and Minitti, S. A. 1984. Esquema de la evolución geodinámica de la Cuenca Neuquina y sus implicancias paleogeográficas. *In* 9th Congreso Geológico Argentino (San Carlos de Bariloche, 1984), Actas. Buenos Aires, Asociación Geológica Argentina, 2:147–162.
Duarte, L. V. 2007. Lithostratigraphy, sequence stratigraphy and depositional setting of the Pliensbachian and Toarcian series in the Lusitanian Basin, Portugal. Cienc. Terra (UNL) 16:17–23.
Eppinger, K. J., and Rosenfeld, U. 1996. Western margin and provenance of sediments in the Neuquén Basin (Argentina) in the Late Jurassic and Early Cretaceous. Tectonophysics 259:229–244.
Feraud, G.; Alric, V.; Fornari, M.; Bertrand, H.; and Haller, M. 1999. $^{40}Ar/^{39}Ar$ dating of the Jurassic volcanic province of Patagonia: migrating magmatism related to Gondwana break-up and subduction. Earth Planet. Sci. Lett. 172:83–96.
Fraguas, Á., and Young, J. 2011. Evolution of the coccolith genus *Lotharingius* during the Late Pliensbachian-Early Toarcian interval in Asturias (N Spain). Consequences of the Early Toarcian environmental perturbations. Geobios 44:361–375.
Franzese, J.; Spalletti, L.; Gómez Pérez, I.; and Macdonald, D. 2003. Tectonic and paleoenvironmental evolution of Mesozoic sedimentary basin along the Andean foothills of Argentina (32°–54°S). J. S. Am. Earth Sci. 16:81–90.
Gómez, J. J.; Goy, A.; and Canales, M. L. 2008. Seawater temperature and carbon isotope variations in belemnites linked to mass extinction during the Toarcian (Early Jurassic) in central and northern Spain. Comparison with other European sections. Palaegeogr. Palaeoclimatol. Palaeoecol. 258:28–58.
Gradstein, F. M.; Ogg, J. G.; Schmitz, M. D.; and Ogg, G. M. 2012. The geologic time scale 2012. Vol. 2. Elsevier, Oxford.
Gröcke, D. R.; Hori, R. S.; Trabucho-Alexandre, J.; Kemp, D. B.; and Schwark, L. 2011. An open marine record of the Toarcian oceanic anoxic event. Solid Earth 2:245–257.
Guex, J.; Blair, S.; Bartolini, A.; Spangenberg, J.; Schaltegger, U.; O'Dogherty, L.; Taylor, D.; Bucher, H.; and Atudorei, V. 2012. Geochronological constraints on post-extinction recovery of the ammonoids and carbon cycle perturbations during the Early Jurassic. Palaeogeogr. Palaeoclimatol. Palaeoecol. 346–347:1–11.
Gulisano, C. A., and Gutiérrez Pleimling, A. R. 1995*a*. Field guide: the Jurassic of the Neuquén Basin. a. Neuquén Province. Ser. E, No. 2. Buenos Aires, Asociación Geológica Argentina, 111 p.
———. 1995*b*. Field guide: the Jurassic of the Neuquén Basin. b. Mendoza Province. Ser. E, No. 3. Buenos Aires, Asociación Geológica Argentina, 103 p.
Hallam, A. 1981. A revised sea-level curve for the early Jurassic. J. Geol. Soc. Lond. 138:735–743.
———. 1988. A re-evaluation of the Jurassic eustasy in the light of new data and the revised Exxon curve. *In* Wilgus, C. K.; Hastings, B. S.; Posamentier, H. W.; van Wagoner, J. C.; Ross, C. A.; and Kendall, C. G. St. C.,

eds. Sea-level changes: an integrated approach. SEPM Spec. Publ. 42:261–273. Tulsa, OK, Society of Economic Paleontologists and Mineralogists.

Hermoso, M.; Le Callonnec, L.; Minoletti, F.; Renard, M.; and Hesselbo, S. P. 2009. Expression of the Early Toarcian negative carbon-isotope excursion in separated carbonate microfractions (Jurassic, Paris Basin). Earth Planet. Sci. Lett. 277:194–203.

Hermoso, M.; Minoletti, F.; Rickaby, R. E. M.; Hesselbo, S. P.; Baudin, F.; and Jenkyns, H. 2012. Dynamics of a stepped carbon-isotope excursion: ultra high-resolution study of early Toarcian environmental change. Earth Planet. Sci. Lett. 319–320:45–54.

Hesselbo, S. P. 2008. Sequence stratigraphy and inferred relative sea-level change from the onshore British Jurassic. Proc. Geol. Assoc. 119:19–34.

Hesselbo, S. P.; Gröcke, D. R.; Jenkyns, H. C.; Bjerrum, C. J.; Farrimond, P.; Morgans Bell, H. S.; and Green, O. R. 2000. Massive dissociation of gas hydrate during a Jurassic oceanic anoxic event. Nature 406:392–395.

Hesselbo, S. P., and Jenkyns, H. C. 1998. British Lower Jurassic sequence stratigraphy. *In* de Graciansky, P.-C.; Hardenbol, J.; Jacquin, T.; and Vail, P. R., eds. Mesozoic and Cenozoic sequence stratigraphy of European basins. SEPM Spec. Publ. 60:561–581. Tulsa, OK, Society of Economic Paleontologists and Mineralogists.

Hesselbo, S. P.; Jenkyns, H. C.; Duarte, L. V.; and Oliveira, L. C. V. 2007. Carbon-isotope record of the Early Jurassic (Toarcian) oceanic anoxic event from fossil wood and marine carbonate (Lusitanian Basin, Portugal). Earth Planet. Sci. Lett. 253:455–470.

Hesselbo, S. P., and Pieńkowski, G. 2011. Stepwise atmospheric carbon-isotope excursion during the Toarcian oceanic anoxic event. Earth Planet. Sci. Lett. 301:365–372.

Howarth, M. K. 1992. The ammonite family Hildoceratidae in the lower Jurassic of Britain. Pt. 2. Monogr. Palaeontogr. Soc. Lond. 146:107–200.

Iglesia Llanos, M. P., and Riccardi, A. C. 2000. The Neuquén composite section: magnetostratigraphy and biostratigraphy of the marine lower Jurassic from the Neuquén Basin (Argentina). Earth Planet. Sci. Lett. 181:443–457.

Iglesia Llanos, M. P.; Riccardi, A. C.; and Singer, E. S. 2006. Palaeomagnetic study of lower Jurassic marine strata from the Neuquén Basin, Argentina: a new Jurassic apparent polar wander path for South America. Earth Planet. Sci. Lett. 252:379–397.

Ikeda, M., and Hori, R. S. 2014. Effects of Karoo-Ferrar volcanism and astronomical cycles on the Toarcian oceanic anoxic events Early Jurassic. Palaeogeogr. Palaeoclimatol. Palaeoecol. 410:134–142.

Ikeda, M., and Tada, R. 2014. A 70 million year astronomical time scale for the deep-sea bedded chert sequence (Inuyama, Japan): implications for the Triassic-Jurassic geochronology. Earth Planet. Sci. Lett. 399: 30–43.

Jahren, A. H.; Arens, N. C.; Sarmiento, G.; Guerrero, J.; and Amundson, R. 2001. Terrestrial record of methane hydrate dissociation in the Early Cretaceous. Geology 29:159–162.

Jefferies, R., and Minton, P. 1965. The mode of life of two Jurassic species of "*Posidonia*" (Bivalvia). Palaeontology 8(1):156–185.

Jenkyns, H. C. 1988. The early Toarcian (Jurassic) anoxic event: stratigraphic, sedimentary and geochemical evidence. Am. J. Sci. 288:101–151.

———. 2003. Evidence for rapid climate change in the Mesozoic-Palaeogene greenhouse world. Philos. Trans. R. Soc. A 231:1885–1916.

———. 2010. Geochemistry of oceanic anoxic events. Geochem. Geophys. Geosyst. 11:Q03004. doi:10.1029/2009GC002788.

Jenkyns, H. C., and Clayton, C. J. 1986. Black shales and carbon isotopes in pelagic sediments from the Tethyan lower Jurassic. Sedimentology 33:87–106.

———. 1997. Lower Jurassic epicontinental carbonates and mudstones from England and Wales: chemostratigraphic signals and the early Toarcian anoxic event. Sedimentology 44:687–706.

Jenkyns, H. C.; Gröcke, D. R.; and Hesselbo, S. P. 2001. Nitrogen isotope evidence for water mass denitrification during the early Toarcian (Jurassic) oceanic anoxic event. Paleoceanography 16:593–603.

Jenkyns, H. C.; Jones, C. E.; Gröcke, D. R.; Hesselbo, S. P.; and Parkinson, D. N. 2002. Chemostratigraphy of the Jurassic system: applications, limitations, and implications for palaeoceanography. J. Geol. Soc. Lond. 159:351–378.

Jones, C. E., and Jenkyns, H. C. 2001. Seawater strontium isotopes, oceanic anoxic events, and seafloor hydrothermal activity in the Jurassic and Cretaceous. Am. J. Sci. 301:112–149.

Jourdan, F.; Féraud, G.; Bertrand, H.; Watkeys, M. K.; and Renne, P. R. 2008. The $^{40}Ar/^{39}Ar$ ages of the sill complex of the Karoo large igneous province: implications for the Pliensbachian-Toarcian climate change. Geochem. Geophys. Geosyst. 9:Q06009. doi:10.1029/2008GC001994.

Kafousia, N.; Karakitsios, V.; Jenkyns, H. C.; and Mattioli, E. 2011. A global event with a regional character: the early Toarcian oceanic anoxic event in the Pindos Ocean (northern Peloponnese, Greece). Geol. Mag. 148:619–631.

Kemp, D. B.; Coe, A. L.; Cohen, A. S.; and Schwark, L. 2005. Astronomical pacing of methane release in the Early Jurassic period. Nature 437:396–399.

Kemp, D. B., and Izumi, K. 2014. Multiproxy geochemical analysis of a Panthalassic margin record of the early Toarcian oceanic anoxic event (Toyora area, Japan). Palaeogeogr. Palaeoclimatol. Palaeoecol. 414:332–341.

Kump, L. R.; Bralower, T. J.; and Ridgwell, A. 2009. Ocean acidification in deep time. Oceanography 22:94–107.

Küspert, W. 1982. Environmental changes during oil shale deposition as deduced from stable isotope ratios. *In* Einsele, G., and Seilacher, A., eds. Cyclic and event stratification. Berlin, Springer, p. 482–501.

Lanés, S. 2005. Late Triassic to Early Jurassic sedimentation in northern Neuquén Basin, Argentina: tectosedimentary evolution of the first transgression. *In* Riccardi, A. C., ed. New insights into the Jurassic record of South America (Andes and Patagonia). Geol. Acta 3(2):81–106.

Leanza, H. A.; Mazzini, A.; Corfu, F.; Llambías, E. J.; Svensen, H.; Planke, S.; and Galland, O. 2013. The Chachil Limestone (Pliensbachian–earliest Toarcian) Neuquén Basin Argentina: U-Pb age calibration and its significance on the Early Jurassic evolution of southwestern Gondwana. J. S. Am. Earth Sci. 42:171–185.

Legarreta, L., and Uliana, M. A. 1996. The Jurassic succession in west-central Argentina: stratal patterns, sequences and paleogeographic evolution. Palaeogeogr. Palaeoclimatol. Palaeoecol. 120:303–330.

Littler, K.; Hesselbo, S. P.; and Jenkyns, H. C. 2010. A carbon-isotope perturbation at the Pliensbachian-Toarcian boundary: evidence from the Lias Group, NE England. Geol. Mag. 147:181–192.

Manceñido, M. O. 1990. The succession of Early Jurassic brachiopod faunas from Argentina: correlations and affinities. *In* MacKinnon, D. I.; Lee, D. E.; and Campbell, J. D., eds. Brachiopods through time: proceedings of the 2nd International Brachiopod Congress (Dunedin). Rotterdam, Balkema, p. 397–404.

Mattioli, E., and Erba, E. 1999. Synthesis of calcareous nannofossil events in Tethyan lower and middle Jurassic successions. Riv. Ital. Paleontol. Stratigr. 105:343–376.

Mazzini, A.; Svensen, H.; Leanza, H. A.; Corfu, F.; and Planke, S. 2010. Early Jurassic shale chemostratigraphy and U-Pb ages from the Neuquén Basin (Argentina): implications for the Toarcian oceanic anoxic event. Earth Planet. Sci. Lett. 297:633–645.

McElwain, J. C.; Wade-Murphy, J.; and Hesselbo, S. P. 2005. Changes in carbon dioxide during an oceanic anoxic event linked to intrusion into Gondwana coals. Nature 435:479–482.

Méhay, S.; Keller, C. E.; Bernasconi, S. M.; Weissert, H.; Erba, E.; Bottini, C.; and Hochuli, P. A. 2009. A volcanic CO_2 pulse triggered the Cretaceous oceanic anoxic event 1a and a biocalcification crisis. Geology 37:819–822.

Monteiro, F. M.; Pancost, R. D.; Ridgwell, A.; and Donnadieu, Y. 2012. Nutrients as the dominant control on the spread of anoxia and euxinia across the Cenomanian-Turonian oceanic anoxic event (OAE2): model-data comparison. Paleoceanography 27:PA4209. doi:10.1029/2012PA002351.

Nullo, F. E.; Stephens, G.; Combina, A.; Dimieri, L.; Balduaf, P.; and Bouza, P. 2005. Malargüe geological map 3569-III/3572/IV: Provincia de Mendoza. Instituto de Geología y Recursos Minerales, Bol. 346. Buenos Aires, Servicio Geológico Minero Argentino, 85 p.

Owens, J. D.; Gill, B. C.; Jenkyns, H. C.; Bates, S. M.; Severmann, S.; Kuypers, M. M. M.; Woodfine, R. G.; and Lyons, T. W. 2013. Sulfur isotopes track the global extent and dynamics of euxinia during Cretaceous oceanic anoxic event 2. Proc. Natl. Acad. Sci. USA 110:18407–18412.

Page, K. N. 2004. A sequence of biohorizons for the subboreal province lower Toarcian in northern Britain and their correlation with a submediterranean standard. Riv. Ital. Paleontol. Stratigr. 110:109–114.

Pálfy, J., and Smith, P. L. 2000. Synchrony between Early Jurassic extinction, oceanic anoxic event, and the Karoo-Ferrar flood basalt volcanism. Geology 28:747–750.

Pálfy, J.; Smith, P. L.; and Mortensen, J. K. 2002. Dating the end-Triassic and Early Jurassic mass extinctions, correlative large igneous provinces, and isotopic events. Geol. Soc. Am. Spec. Pap. 356:523–532.

Pancost, R. D.; Crawford, N.; Magness, S.; Turner, A.; Jenkyns, H. C.; and Maxwell, J. R. 2004. Further evidence for the development of photic-zone euxinic conditions during Mesozoic oceanic anoxic events. J. Geol. Soc. Lond. 161:353–364.

Pankhurst, R. J.; Leat, P. T.; Sruoga, P.; Rapela, C. W.; Márquez, M.; Storey, B. C.; and Riley, T. R. 1998. The Chon Aike province of Patagonia and related rocks in West Antarctica: a silicic large igneous province. J. Volcanol. Geotherm. Res. 81:113–136.

Pasley, M. A.; Gregory, W. A.; and Hart, G. F. 1991. Organic matter variations in transgressive and regressive shales. Organic Geochem. 17:483–509.

Percival, L. M. E.; Witt, M. L. I.; Mather, T. A.; Hermoso, M.; Jenkyns, H. C.; Hesselbo, S. P.; Al-Suwaidi, A. H.; Storm, M. S.; Xu, W.; and Ruhl, M. 2015. Globally enhanced mercury deposition during the end-Pliensbachian extinction and Toarcian OAE: a link to the Karoo-Ferrar large igneous province. Earth Planet. Sci. Lett. 428:267–280.

Ramos, V. A.; Niemeyer, H.; Skarmeta, J.; and Muñoz, J. 1982. Magmatic evolution of the Austral Patagonian Andes. Earth Sci. Rev. 18:411–443.

Riccardi, A. C. 1983. The Jurassic of Argentina and Chile. *In* Moullade, M., and Nairn, A. E. M., eds. Phanerozoic geology of the world: the Mesozoic. Pt. B. Amsterdam, Elsevier, p. 201–263.

———. 2005. First teuthid cephalopod from the lower Jurassic of South America (Neuquén Basin, Argentina). *In* Riccardi, A. C., ed. New insights into the Jurassic record of South America (Andes and Patagonia). Geol. Acta 3(2):179–184.

———. 2008*a*. El Jurásico de la Argentina y sus amonites. Rev. Asoc. Geol. Arg. 63:625–643.

———. 2008*b*. The marine Jurassic of Argentina: a biostratigraphic framework. Episodes 31:326–335.

Riccardi, A. C.; Damborenea, S. E.; Manceñido, M. O.; and Leanza, H. A. 2011. Megainvertebrados del Jurásico y su importancia geobiológica. *In* Leanza, H. A.; Arregui, C.; Carbone, O., Danieli, J. C.; and Vallés, J. M., eds. Relatorio del 18 Congreso Geológico Argentino, Neuquén, Argentina, p. 441–464.

Riccardi, A. C., and Kamo, S. 2012. A new U-Pb zircon age for an ash layer at the Pliensbachian-Toarcian boundary, Argentina. *In* Unearthing our past and future—resourcing tomorrow: 34th International Geological Congress (Brisbane, Australia), abstracts. p. 752.

———. 2014. Biostratigraphy and geochronology of the Pliensbachian-Toarcian boundary in Argentina. *In* Re-

súmenes del 19 Congreso Geológico Argentino, Córdoba, Argentina, T-42.
Riccardi, A. C.; Leanza, H. A.; Damborenea, S. E.; Manceñido, M. O.; Ballent, S. C.; and Zeiss, A. 2000. Marine Mesozoic biostratigraphy of the Neuquén Basin. *In* Miller, H., and Hervé, F., eds. Geoscientific cooperation with Latin America: 31st International Geological Congress (Rio de Janeiro, Brazil). Z. Angew. Geol. Sonderh. SH1:103–108.
Richards, M.; Bowman, M.; and Reading, H. 1998. Submarine-fan systems I: characterization and stratigraphic pediction. Mar. Pet. Geol. 15:689–717.
Röhl, H.-J.; Schmid-Röhl, A.; Oschmann, W.; Frimmel A.; and Schwark, L. 2001. The Posidonia Shale (lower Toarcian) of SW-Germany: an oxygen-depleted ecosystem controlled by sea level and paleoclimate. Palaeoceanogr. Palaeoclimatol. Palaeoecol. 165:27–52.
Ros Franch, S.; Marquez-Aliaga, A.; and Damborenea, S. E. 2014. Comprehensive database on Induan (lower Triassic) to Sinemurian (lower Jurassic) marine bivalve genera and their paleobiogeograpic record. Paleontol. Contrib. 8:3–219.
Sabatino, N.; Neri, R.; Bellanca, A.; Jenkyns, H. C.; Baudin, F.; Parisi, G.; and Masetti, D. 2009. Carbon-isotope records of the Early Jurassic (Toarcian) oceanic anoxic event from the Valdorbia (Umbria-Marche Apennines) and Monte Mangart (Julian Alps) sections: palaeoceanographic and stratigraphic implications. Sedimentology 56:1307–1328.
Schlanger, S. O., and Jenkyns, H. C. 1976. Cretaceous oceanic anoxic events: causes and consequences. Geol. Mijnb. 55:179–184.
Schmid-Röhl, A.; Röhl, H.-J.; Oschmann, W.; Frimmel, A.; and Schwark, L. 2002. Palaeoenvironmental reconstruction of lower Toarcian epicontinental black shales (Posidonia Shale, SW Germany): global versus regional control. Geobios 35:13–20.
Schouten, S.; van Kaam-Peters, M. E.; Rijpstra, W. I. C.; Schoell, M.; and Sinninghe Damste, J. S. 2000. Effects of an oceanic anoxic event on the stable carbon isotopic composition of early Toarcian carbon. Am. J. Sci. 300:1–22.
Self, S. 2006. The effects and consequences of very large volcanic eruptions. Philos. Trans. R. Soc. A 364:2073–2097.
Sell, B.; Ovtcharova, M.; Guex, J.; Bartolini, A.; Jourdan, F.; Spangenberg, J. E.; Vicente, J. C.; and Schaltegger, U. 2014. Evaluating the temporal link between the Karoo LIP and climatic-biologic events of the Toarcian Stage with high-precision U-Pb geochronology. Earth Planet. Sci. Lett. 408:48–56.
Suan, G.; Nikitenko, B. L.; Rogov, M. A.; Baudin, F.; Spangenberg, J. E.; Knyazev, V. G.; Glinskikh, L. A.; et al. 2011. Polar record of the Early Jurassic massive carbon injection. Earth Planet. Sci. Lett. 312:102–113.
Svensen, H.; Corfu, F.; Polteau, S.; Hammer, Ø.; and Planke, S. 2012. Rapid magma emplacement in the Karoo large igneous province. Earth Planet. Sci. Lett. 325–326:1–9.
Svensen, H.; Planke, S.; Chevallier, L.; Malthe-Sørenssen, A.; Corfu, F.; and Jamtveit, B. 2007. Hydrothermal venting of greenhouse gases triggering Early Jurassic global warming. Earth Planet. Sci. Lett. 256:554–566.
Tissot, B.; Durand, B.; Espitalié, J.; and Combaz, A. 1974. Influence of nature and diagensis of organic matter in formation of petroleum. Am. Assoc. Pet. Geol. Bull. 58:499–506.
Valencio, S. A.; Cagnoni, M. C.; Ramos, A. M.; Riccardi, A. C.; and Panarello, H. O. 2005. Chemostratigraphy of the Pliensbachian, Puesto Araya Formation (Neuquén Basin, Argentina). *In* Riccardi, A. C., ed. New insights into the Jurassic record of South America (Andes and Patagonia). Geol. Acta 3(2):147–154.
Vergani, G. D.; Tankard, A. J.; Belotti, H. J.; and Welsink, H. J. 1995. Tectonic evolution and paleogeography of the Neuquén Basin, Argentina. *In* Tankard, A. J.; Suárez Soruco, R.; and Welsink, H. J., eds. Petroleum basins of South America. Am. Assoc. Pet. Geol. Mem. 62:383–402.
Vicente, J. C. 2005. Dynamic paleogeography of the Jurassic Andean Basin: pattern of transgression and localisation of main straits through the magmatic arc. Rev. Asoc. Geol. Arg. 60:221–250.
Volkheimer, W. 1973. Palinología estratigráfica del Jurásico de la Sierra de Chacai Có y adyacencias (Cuenca Neuquina, República Argentina). I. Estratigrafía de las Formaciones Sierra Chacai Có (Pliensbachiano), Los Molles (Toarciano, Aaleniano), Cura Niyeu (Bayociano) y Lajas (Caloviano inferior). Ameghiniana 10:105–131.
von Hillebrandt, A. 1973. Die Ammonitengattungen *Bouleiceras* und *Frechiella* im Jura von Chile. Eclogae Geol. Helv. 66:351–363.
———. 1987. Liassic ammonite zones of South America and correlations with other provinces: with description of new genera and species of ammonites. *In* Volkheimer, W., ed.: Bioestratigrafía de los sistemas regionales del Jurásico y Cretácico de América del Sur. Mendoza, Argentina, Comité Sudamericano del Jurásico y Cretácico, p. 111–157.
———. 2006. Ammoniten aus dem Pliensbachium (Carixium und Domerium) von Südamerika. Rev. Paleobiol. 25:1–403.
von Hillebrandt, A., and Schmidt-Effing, R. 1981. Ammoniten aus dem Toarcium (Jura) von Chile (Südamerika). Zitteliana 6:3–74.
von Hillebrandt, A.; Smith, P.; Westermann, G. E. G.; and Callomon, J. H. 1992. Ammonite zones of the circum-Pacific region. *In* Westermann, G. E. G., ed. The Jurassic of the circum-Pacific. Cambridge, Cambridge University Press, p. 247–272.
Wignall, P. B.; McArthur, J. M.; Little, C. T. S.; and Hallam, A. 2006. Methane release in the Early Jurassic period. Nature 441:E5.